Integrability and Chaos via fractal analysis of Spectral Form Factors:
Gaussian approximations and exact results

Lorenzo Campos Venuti[1,2,*], Jovan Odavić[1,3] and Alioscia Hamma[1,3,4]

[1]*Dipartimento di Fisica 'Ettore Pancini', Università degli Studi di Napoli Federico II, Via Cintia 80126, Napoli, Italy*
[2]*Department of Physics and Astronomy, University of Southern California, Los Angeles, USA*
[3]*Istituto Nazionale di Fisica Nucleare (INFN), Sezione di Napoli, Italy*
[4]*Scuola Superiore Meridionale, Largo S. Marcellino 10, 80138 Napoli, Italy*

We establish the mathematical equivalence between the spectral form factor, a quantity used to identify the onset of quantum chaos and scrambling in quantum many-body systems, and the classical problem of statistical characterization of planar random walks. We thus associate to any quantum Hamiltonian a random process on the plane. We set down rigorously the conditions under which such random process becomes a Wiener process in the thermodynamic limit and the associated distribution of the distance from the origin becomes Gaussian. This leads to the well known Gaussian behavior of the spectral form factor for quantum chaotic (non-integrable) models, which we show to be violated at low temperature. For systems with quasi-free spectrum (integrable), instead, the distribution of the SFF is Log-Normal. We compute all the moments of the spectral form factor exactly without resorting to the Gaussian approximation. Assuming degeneracies in the quantum chaotic spectrum we solve the classical problem of random walker taking steps of unequal lengths. Furthermore, we demonstrate that the Hausdorff dimension of the frontier of the random walk, defined as the boundary of the unbounded component of the complement, approaches 1 for the 'integrable' Brownian motion, while the non-integrable walk approaches that obtained by the Schramm-Loewner Evolution (SLE) with the fractal dimension 4/3. Additionally, we numerically show that 'Bethe Ansatz' walkers fall into a category similar to the non-integrable walkers.

I. INTRODUCTION

The spectral form factor (SFF) $S(t)$ has the form

$$S(t) = |\chi(t)|^2, \ \chi(t) = \text{tr}\left(\rho e^{-itH}\right), \tag{1}$$

where H is the Hamiltonian under consideration and ρ is a possibly not normalized quantum state. The number of interesting physical problems that can be written, often exactly, in this form, either quantum or classical, is frankly quite amazing. Lagrange showed that the study of the motion of perihelia is connected to the argument of an expression like $\chi(t)$ with $\rho = \mathbb{1}$ [1]. For a pure quantum state $\rho = |\psi\rangle\langle\psi|$, $S(t)$ is known as Loschmidt echo or survival probability and is connected to the theory of Fermi-edge singularity in metals [2], the statistics of the work done after a quench [3], the approach to thermodynamic equilibrium [4–6] and (especially for $\rho = 1$) quantum chaos [7–16]. More recently, the SFF has found applications in quantum gravity [17–19]. Using the SYK as a model for a black hole, the late-time behavior of the SFF probes the discreteness of the black hole spectrum. Three regimes have been identified for the SFF. A short-time regime (the "slope") where $S(t)$ is observed to be self-averaging, a long time "plateau" where $S(t)$ is approximately constant but subject to large fluctuations, and an intermediate regime connecting the two (the "ramp"). It was recognized already in [4, 20] that a cumulant expansion implies $S(t) \simeq e^{-(\langle H^2\rangle - \langle H\rangle^2)t^2}$ for short times, which, due to the self-averaging property of the SYK moments $\langle H^{2p}\rangle$, implies the observed universal short-time regime. For larger time the cumulant expansion breaks down and $S(t)$ start oscillating erratically. It is exactly this challenging regime we shall put more emphasis here. It has been known for quite some time that the value of the plateau is related to a particular Gaussian approximation [14, 21] (we will come back to this point below).

Yet another way to look at Eq. (1) is as the position of a random walker on the complex plane. This analogy was first utilized by Rayleigh [22, 23] and the celebrated Rayleigh distribution is precisely the distribution of the distance of the walker from the origin $|\chi(t)|$, under the above mentioned Gaussian approximation.

In this paper, we further exploit the random walk analogy. The entire path of the walker is seen as a random process of discrete time, of which $|\chi(t)|$ represents the modulus of the last position. We set down rigorously the conditions under which the Gaussian approximation for $|\chi(t)|$ is legitimate. We show that these hypotheses are generally satisfied in the high-temperature phase, but fail at low temperature and for $\rho = |\psi\rangle\langle\psi|$ for a small quench at a critical point. Under similar hypotheses, the entire path becomes a 2D Wiener process in a precise scaling limit. The properties of the random walk, seen as a fractal, reflect

---
[*] Corresponding author: lorenzo.camposvenuti@unina.it
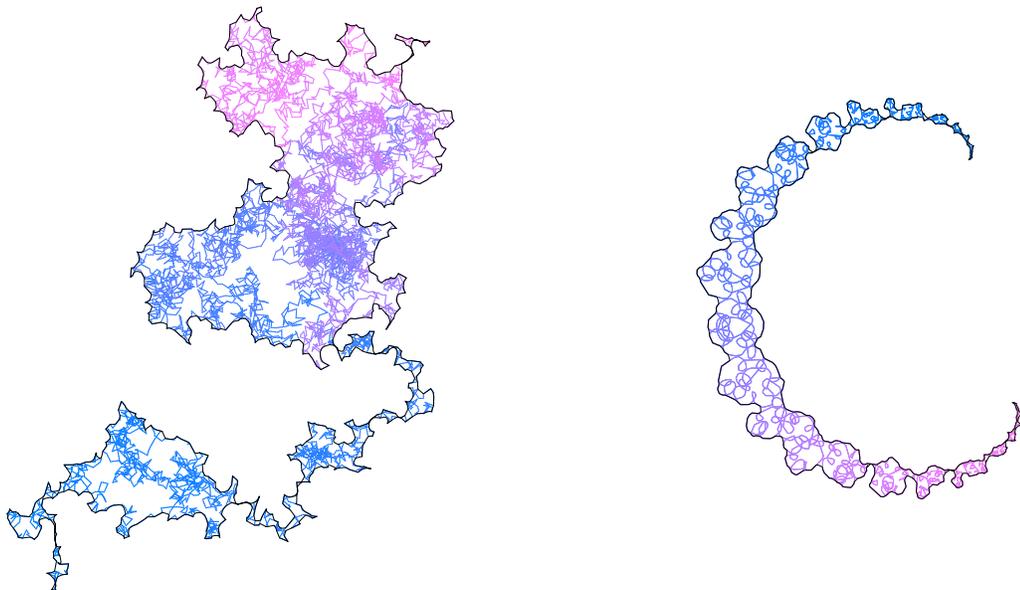
Figure 1. Fractals and their frontiers, in black, corresponding to physical models: non-integrable (left) vs integrable (right). Color from blue to pink corresponds to increasing time-steps of the random walks. The frontier is essentially the boundary of the fractal without the inner islands, see text for details. The non-integrable Hamiltonian is the XXZ model with next nearest neighbor interactions (see Eq. (21)), with $(\Delta, \alpha) = (0.4, 0.5)$. The integrable Hamiltonian is the XY model with parameters $(h, \gamma) = (0.2, 0.3)$; see Appendix H 6.

the integrability or lack thereof of the Hamiltonian H. In particular, our numerics for non-integrable models, show that the dimension of the frontier of the random walk is close to $4/3$, which is the value expected for the Wiener process, while it is close to 1 for quasi-free systems.

While, in the generic non-integrable case, $|\chi(t)|$ is a sum of independent variables, for quasi-free models, $|\chi(t)|$ is rather a product of independent variables and its distribution is log-normal. Finally, we also give the exact expression for the moments of the SFF beyond the Gaussian approximation as a closed-form recursion and in full generality accounting for possible degeneracies in the spectrum. These exact results extend, in the plateau region, the beyond-Gaussian approximation obtained in the ramp-plateau regime of [16] (see also [24–30]), and can serve as a check for further approximations on the time dependence of the SFF.

II. THE FRACTAL GEOMETRY OF SPECTRAL STATISTICS

For each "system size" L, we assume the Hamiltonian H lives in a Hilbert space of dimension D e.g. for qubits $D = 2^L$. We allow the Hamiltonian to have degenerate eigenvalues. Indeed, general physical models, even non-integrable, chaotic ones, possess several symmetries and degeneracies. Using the spectral resolution of the Hamiltonian, $H = \sum_{j=1}^{N_B} E_j \Pi_j$ (E_j eigenenergies, Π_j eigenprojectors, N_B the number of blocks) we have, with $d_j = \text{tr}(\rho \Pi_j) > 0$,

$$\chi(t) = \sum_{j=1}^{N_B} d_j e^{-itE_j}. \tag{2}$$

We now show how to associate to any pair (H, ρ) a random walk on the plane. In this way, we encode information about the pair (H, ρ) into a single function, more precisely into a stochastic process. This analogy has already been used in [21] but we are going to follow its consequences further. For each system size L we diagonalize the Hamiltonian H and obtain the sets $\left(\{E_j\}^\uparrow, \{d_j\}\right)$ of ascending eigenvalues $E_1 < E_2 < \cdots < E_{N_B}$. Time t is a random variable acted upon by the following expectation value,

$$\overline{f(t)} := \lim_{T \to \infty} \frac{1}{T} \int_0^T dt f(t), \tag{3}$$

in other words, in the spirit of ergodic theory and statistical mechanics, time is subject to infinite time average. We thus obtain an ensemble of walks on the plane, indexed by a random variable t, i.e. a random walk. At step n the walker is at position

$Z_n(t) = \sum_{j=1}^n d_j e^{-itE_j}$ on the complex plane ($Z_0(t) = 0$), $n = 1, 2, \ldots, N_B$. At step $n + 1$ the walker rotates clockwise by an angle tE_{n+1} and takes a step of length d_{n+1}. For each L we only have a walker with a finite (albeit exponentially large) number of steps, and we are naturally interested in what happens in the thermodynamic limit when $L \to \infty$. Note that the path of the walker is strongly dependent on the ordering of the energies. Our natural ordering is consistent with the analogous choice in random matrix theory (RMT).

Unlike the more familiar random walks defined on a lattice, this walker can occupy any point on the complex plane $\simeq \mathbb{R}^2$.[1] A useful quantity to describe a random walk is the probability that the walker is at position $\boldsymbol{z} = (z_1, z_2)$ after n steps. Since the points $\boldsymbol{z}$ form a continuum we have the following probability density

$$P_{Z_n}(\boldsymbol{z}) = \overline{\delta\left(z_1 - \mathrm{Re}(Z_n(t))\right) \delta\left(z_2 - \mathrm{Im}(Z_n(t))\right)}. \tag{4}$$

In particular, the even moments of the distance of the walker from the origin

$$I_m := \overline{|\chi(t)|^{2m}} \tag{5}$$

have been the subject of intense research efforts [29, 31–33]. As we will see, these quantities correspond to the long time plateau studied in random matrix theory. More precisely, in the context of RMT the following quantity has been studied: $\mathsf{E}_x\left[|\chi_x(t)|^{2m}\right]$, where we indicate with x the collection of random variables, χ_x denotes that χ depends on the particular realization x, and $\mathsf{E}_x\left[\bullet\right]$ is the ensemble average. The connection between I_m of Eq. (5) and $\mathsf{E}_x\left[|\chi_x(t)|^{2m}\right]$ studied in RMT is given by the following result (see Appendix A for a proof and Sec. 4.5 of [34] for a similar result):

Theorem 1. *Let $H(x)$ be a Hamiltonian dependent on the random variables x. If the induced distribution $\mu_{\boldsymbol{E}}(d\boldsymbol{E})$ of the eigenvalues of $H(x)$ is absolutely continuous, and $\mathrm{tr}\left(\Pi_j(x)\right)$ and $d_j(x)$ do not depend on x, the ensemble average and time average commute and one has:*

$$\lim_{t \to \infty} \mathsf{E}_x\left[|\chi_x(t)|^{2m}\right] = \overline{\mathsf{E}_x\left[|\chi_x(t)|^{2m}\right]}$$
$$\mathsf{E}_x\left[\overline{|\chi_x(t)|^{2m}}\right] = \overline{|\chi_x(t)|^{2m}}. \tag{6}$$

The last equation means that infinite time moments are independent of the specific realization x. All the hypotheses are very natural for random models, in particular if degeneracies exist, they should not depend on the random variables. This result applies, for example, to the SYK model at infinite temperature ($\rho = \mathbb{1}$) [2] and means that the value of the moments of the SFF, the plateaus, can be obtained also taking the infinite time average and even over a single realization.

So far, the random-walk interpretation of the spectral form factor provides a perhaps amusing physical analogy, but there are other tools that can be used to analyze a random walk. In general, the trajectory formed by a random walk is a fractal: a geometrical object whose Hausdorff dimension can assume non-integer values. To gain some insight let us consider the familiar random walk on a two-dimensional square lattice. At each step, the walker chooses one out of the four possible directions uniformly at random. In the scaling limit, where the number of steps goes to infinity and the lattice spacing goes to zero (in a precise way), the random walk becomes a Wiener process [3], for which it can be proven that the fractal dimension is two with probability one [35]. Another interesting geometrical feature of a fractal is its frontier, which is defined as follows. Let K be a compact, connected set of the plane. The complement of K has one unbounded component and its boundary is the frontier of K. Intuitively the frontier of a set is the boundary without the inner islands. Mandelbrot conjectured in 1982 that the fractal dimension of the frontier of the Wiener process is 4/3 [36]. This was rigorously proved in 2001 using methods of stochastic Loewner evolution [37]. Our aim here is to study the pair (H, ρ) using methods of fractal geometry, in particular studying the dimension of the frontier of its corresponding random walk. As we will show, for independent spectra $\{E_j\}$ and *generic* weights d_j to be defined momentarily, the scaling limit of its associated random walk becomes a Wiener process in the thermodynamic limit. We begin by computing the probability distribution of the position Eq. (4), or rather its renormalized form $Y_n = Z_n/\Delta Z_n$ where $(\Delta Z_n)^2 = \overline{|Z_n(t)|^2}$, which can be readily shown to be equal to $(\Delta Z_n)^2 = \sum_{j=1}^n d_j^2$.

We say that the spectrum of H is *independent* if the energies $\{E_j\}$ are linearly independent over the rationals. Proving that a certain set of numbers is independent can be a mathematically daunting task. As an extreme example, it is not yet known whether the single-qubit spectrum, $\{1, \gamma_C\}$, where γ_C is the Euler-Mascheroni constant, is independent or not. However, in general, adding a tiny amount of randomness makes the spectrum independent with probability one [38]. For example, the

---

[1] We move from $\mathbb{C}$ to $\mathbb{R}^2$ whichever is more convenient.

[2] In principle we don't know if the eigenvalues distribution is absolutely continuous. Several numerical calculations and the computations in [33] suggest that this is the case.

[3] Random walk, Brownian motion and Wiener process are sometimes all considered synonym. In 1827 Brownian motion was observed by botanist R. Brown in minute particles suspended in liquids. Wiener constructed the "Wiener process" in 1923 as a mathematical model of Brownian motion.

classical ensembles of random matrices, such as GUE, GOE and so on, have independent spectrum almost surely. If the energies are independent, as t increases, the phases tE_j in Eq. (2) fill the torus $\mathbb{T}^n$ densely and uniformly, so Z_n becomes a sum of n complex i.i.d. random variables whose phases are distributed uniformly in $[0, 2\pi)$. It is natural to expect that for large n the distribution of Z_n will be Gaussian. This is indeed the case, provided a certain technical condition holds. This condition roughly ensures that a sufficient number of weights d_j are of the same order of magnitude so that the central limit theorem (CLT) can be established.

We say that the weights $\{d_j\}$ are *generic* if they satisfy the following Lyapunov condition, i.e. there exist a $q > 1$ such that

$$\lim_{n\to\infty} R_q^n = 0\,, \quad \text{with } R_q^n := \frac{\sum_{j=1}^n d_j^{2q}}{\left(\sum_{j=1}^n d_j^2\right)^q}\,. \tag{7}$$

Note that, for example, for $\rho = \mathbb{1}$ and if the Hamiltonian spectrum is non-degenerate $d_j = 1\, \forall j$, one gets $R_q^n = n^{-(q-1)}$ and Eq. (7) holds trivially for all $q > 1$. For generic spectra, the weights d_j control the variance of each independent variable. Each variance however depends (possibly also) on n through L. This introduces a sort of "correlation" among the random variables and we cannot simply use the Lyapunov CLT. However for our specific case one can still prove Gaussianity. Indeed, one can show that Eq. (7) implies $R_p^n \to 0$ for all $p > 1$, which in turn implies that all the cumulants of Y_n beyond the second tend to zero implying Gaussianity. The details are shown in Appendix B.

Theorem 2. *For independent spectrum $\{E_j\}$ if the weights $\{d_j\}$ are generic the multivariate probability distribution of the rescaled variable Y_n tends to a standard 2D Gaussian in the thermodynamic limit, i.e.*

$$\lim_{L\to\infty} P_{Y_n}(\boldsymbol{y}) = \frac{1}{\pi} e^{-\|\boldsymbol{y}\|^2}\,. \tag{8}$$

The converse also holds: if the weights are not generic the limiting distribution is not Gaussian.

Theorem 2 has several consequences: i) The moments of the squared renormalized distance $\overline{|Y_n|^{2q}}$ approach $q!$ in the thermodynamic limit, and, which is the same: ii) The distribution of the square distance tends to $P_{|Y_n|^2}(r) = \vartheta(r)e^{-r}$, i.e. $|Y_n|^2 \overset{L\to\infty}{\longrightarrow} \mathrm{Exp}(1)$. iii) The distance itself follows a Rayleigh distribution $P_{|Y_n|}(\rho) \to \vartheta(\rho)2\rho e^{-\rho^2}$ (with moments $\overline{|Y_n|^q} = \Gamma(1 + q/2)$). iv) At finite size the unscaled variable Z_n is approximately distributed as

$$P_{Z_n}(\boldsymbol{z}) \simeq \frac{1}{\pi \Delta Z_n^2} e^{-\|\boldsymbol{z}\|^2/(\Delta Z_n^2)}\,. \tag{9}$$

v) If all the weights $d_j = 1$, $\Delta Z_n^2 =$ number of steps $= n$. This is the essential ingredient of the Brownian motion/Wiener process: the average distance at time n is proportional to $\sqrt{n}$ [4].

There are essentially two ways to violate the Lyapunov condition: a) one can have $|\{d_j > \epsilon\}| = M$ where ϵ is a (tiny) threshold and M a "small" number. This implies that Y_n, in practice, is a sum of only M independent variables and the CLT is violated; b) One can have the variances of each random variable conspire such that the cumulants of Y_n tend to a non-zero value. Condition a) happens, for example, when $\rho = e^{-\beta H}/Z$ at very low temperature when only the lowest energy states are populated. We show evidence of this effect in the SYK model in Appendix H 5. At high temperature the distribution of $|Y_n|^2$ is $\mathrm{Exp}(1)$ in accordance with Theorem 2 while at very low temperature the distribution becomes double peaked signaling a violation of the Lyapunov condition. Condition b) happens, for example, for $d_j = (j/n)^{-\alpha}$ for $\alpha > 1/2$. In this case the ratios converge to universal constants $R_q^n \to \zeta(2q\alpha)/\zeta(2\alpha)^q$ where $\zeta(z)$ is the Riemann zeta function (see [6] for more details). This situation is (highly) unlikely when d_j is simply the degeneracy of level E_j ($\rho = \mathbb{1}$), but becomes possible at finite temperature $\rho = e^{-\beta H}$. In case $\rho = |\psi\rangle\langle\psi|$, such violation of the CLT is obtained by a *small quench* performed at a quantum critical point of H as was detailed in [6, 39, 40]. Very briefly, the small quench condition is the following. Let $H(\lambda) = H_0 + \lambda V$ be a Hamiltonian describing a system of finite linear size L with a quantum critical point at λ_c. The ground state of $H(\lambda_c)$ is precisely $|\psi\rangle$ and the Hamiltonian under consideration is $H(\lambda)$ with $\delta\lambda = |\lambda - \lambda_c| \ll L^{-1/\nu}$ where ν is the correlation length critical exponent. More details can be found in [6, 39, 40].

Note also that when d_j is the degeneracy of level j, both cases above are extremely unlikely in RMT. For example, $d_j = 1$ for the classical random matrix ensembles (GUE, GOE, etc.) with probability one, while for the SYK model $d_j = 1, (2)$ depending on whether $N \mod 8 = 0$ (or not) (see Appendix H 1).

---

[4] Indeed changing variables to $s = n\tau$, $\boldsymbol{x}(s) = aZ_n$, (s has units of time and $\boldsymbol{x}$ of space) in the scaling limit $a, \tau \to 0$ with $a^2/\tau = 2D$ constant, $P_{Z_n}(\boldsymbol{z})$ becomes $P(\boldsymbol{x}, s) = (4\pi Ds)^{-1} \exp(-\|\boldsymbol{x}\|^2/(4Ds))$, the familiar Green's function of diffusion (or heat) equation.

Motivated by the remark v) above, we now investigate if and under what conditions, the above random walk becomes a Wiener process in the scaling limit. More precisely, we define the scaling limit by considering the following random process:

$$W_s^N = \frac{1}{\Delta Z_N} \sum_{j=1}^{\lfloor Ns \rfloor} d_j e^{-it E_j}, \tag{10}$$

where s is the time variable of the random process. Note that if we fix $N = \alpha N_B$ then s is constrained to $[0, 1/\alpha]$ but other choices are possible that result in s being defined on a larger set. To check whether W_s^N defines a two dimensional Wiener process W_s in the limit $N \to \infty$, one should check (see e.g. [35]): a) That the paths have *independent increments*, that is, $W_{s_2} - W_{s_1}$ and $W_{s_4} - W_{s_3}$ are independent if $s_1 \leq s_2 \leq s_3 \leq s_4$; and b) That the distribution of $W_{s+h} - W_s$ is *stationary* (does not depend on s), *isotropic* (does not depend on direction) and is Gaussian with zero mean such that

$$\text{Prob}\left(W : |W_{s+h} - W_s| \leq \rho\right) = \frac{1}{h} \int_0^\rho dr\, r \exp\left(-r^2/(2h)\right). \tag{11}$$

We have the following result.

Theorem 3. *If the spectrum $\{E_j\}$ is independent and the weights $\{d_j\}$ are generic and additionally satisfy the following*

$$\lim_{N \to \infty} R_1^N(h, s) = h, \text{ with } R_1^N(h, s) := \frac{\sum_{k=\lfloor Ns \rfloor + 1}^{\lfloor N(s+h) \rfloor} d_k^2}{\sum_{k=1}^N d_k^2}, \tag{12}$$

then W_s^N converges to a Wiener process as $N \to \infty$.

Indeed, condition a) above is satisfied if the spectrum is generic while condition b) is satisfied provided weights are generic and satisfy Eq. (12) (see Appendix C).

III. EXACT MOMENTS OF THE SPECTRAL FORM FACTOR

After having assessed the Gaussian regime, we now give the exact expression of SFF's moments, which include deviation from Gaussianity. To compute the even moment I_M a weaker hypothesis on the spectrum $\{E_j\}$ than independence is sufficient. We say that the the numbers $\{E_k\}_{k=1}^D$, assumed to be all different, satisfy the non-degeneracy condition at order $M \in \mathbb{N}$ (M-ND) if, for any pair of sequences $\alpha_i, \beta_i \in \{1, 2, \ldots, D\}$, $i = 1, 2, \ldots, M$, the equation

$$\sum_{j=1}^M E_{\alpha_j} = \sum_{j=1}^M E_{\beta_j} \tag{13}$$

implies that $\{\alpha_1, \alpha_2, \ldots, \alpha_M\}$ is a permutation of $\{\beta_1, \beta_2, \ldots, \beta_M\}$, i.e. there exist a permutation $\pi \in \mathbb{S}_M$ such that $\alpha_i = \beta_{\pi(i)}$ for $i = 1, \ldots, M$. In Appendix D we show that the condition M-ND for all $M \in \mathbb{N}$ is equivalent to that of independent spectrum.

As a remark, as we will see in detail below, for non-degenerate spectra notice that one can approximate $I_m \simeq D^m m!$. However, often in literature this is seemingly considered an exact result instead of an approximation [28, 29]. This is manifestly wrong already for $m = 2$ even in the case where $d_j = 1$, as an explicit calculation assuming 2-ND gives $I_2 = 2D^2 - D$. However, if the weights are generic, Theorem 2 shows that, indeed, at leading order in D, $I_m \simeq D^m m!$. Again, this approximation fails for nongeneric weights, for example, in the case $d_j = (j/n)^{-\alpha}$ for $\alpha > 1/2$ or $d_j = \text{tr}\left(e^{-\beta H} \Pi_j\right)$ at very low temperature $1/\beta$.

A correct formula for the case $d_j = 1$ (and independent spectrum) was found in the mathematical literature [31]. Here we give an exact formula valid for general d_j (see Appendix E):

Theorem 4. *Assuming the energies satisfy non-degeneracy at order p, then, for $k = 1, \ldots, p$*

$$I_k = \overline{|\chi(t)|^{2k}} = (k!)^2 \sum_{\sum_{i=1}^{N_B} k_i = k} \prod_{i=1}^{N_B} \left(\frac{d_i^{k_i}}{k_i!}\right)^2. \tag{14}$$

Moreover, defining the coefficients a_n via the series $\ln(I_0(2\sqrt{z})) = \sum_{n=1}^\infty a_n z^n / n!$ and $X_n := \sum_{j=1}^{N_B} (d_j)^{2n}$ one has the following recursion

$$I_p = \sum_{q=1}^{p-1} \binom{p-1}{q-1} \frac{p!}{(p-q)!} a_q X_q I_{p-q} + p! a_p X_p. \tag{15}$$

This theorem offers an exact, iterative, closed-form expression for arbitrary SFF moments beyond the Gaussian approximation. For example, assuming 3-ND, using Eq. (15), one easily obtains

$$I_1 = X_1, I_2 = 2(X_1)^2 - X_2 \tag{16}$$

$$I_3 = 6(X_1)^3 - 9X_1 X_2 + 4X_3. \tag{17}$$

One recognizes a term $m!(X_1)^m$ appearing in I_m corresponding to the Gaussian approximation. For generic weights, this is the leading term in the sense that $\lim_{L \to \infty} I_m / (X_1)^m = m!$ (and so $I_m = m!(X_1)^m + o((X_1)^m)$), but this is no longer true for non-generic weights. In Appendix H 5 we show that formula Eq. (15) always gives the correct moments for the SYK model, while the Gaussian approximation fails at low temperature.

Lastly, we would like to mention that the sequence in Eq. (14) arises in the study of families of Calabi-Yau varieties and the periods of these varieties can be obtained computing recursions for the I_m's, see [41, 42].

IV. INTEGRABLE QUADRATIC MODELS

What happens when the Hamiltonian is integrable? For integrable quadratic Hamiltonians, that is when H is quadratic in either Bosonic or Fermionic creation/annihilation operators, the hypothesis of independent spectrum cannot hold. In fact, the energies of these models have the form $E_{\bm{n}} = \sum_{k=1}^{L} n_k \epsilon_k$ with $n_k = 0, 1$ ($n_k = 0, 1, 2, \ldots$) for Fermions (Bosons) so there can be at most L independent energies (e.g. the one-particle energies). For concreteness, we will stick to the fermionic case in the following. The value of $\chi(t)$ is completely specified by the vector $\varphi(t) := (E_1 t, E_2 t, \ldots, E_{N_B} t) \mod 2\pi$ ($\chi(t) = \sum_{j=1}^{N_B} d_j e^{-i\varphi_j(t)}$). For models with free fermionic spectra, the closure of the trajectory $\varphi(t)$ as t increases is a torus $\mathbb{T}^M$ where $M \leq L$ is the number of independent energies. A relation among the energies is an equation of the form $\sum_j a_j E_j = 0$ with integer a_j. So, quadratic models have at least $D - L$ relations among the energies. Such a large number of relations implies that the steps of the walker are not even approximately independent. In this case we could not compute the probability distribution of the walker Eq. (4) but with mild assumptions we obtained the distribution of $|\chi(t)|^2$ (note that $\chi(t) = Z_{N_B}(t)$). We have the following result:

Theorem 5. *Let H be defined on a 2^L dimensional Hilbert space, have spectrum $E_{\bm{n}} = \sum_{k=1}^{L} n_k \Lambda_k + E_0$ with $n_k = 0, 1$. We allow the one-particle spectrum $\{\Lambda_k\}_{k=1}^{L}$ to have degeneracies, let $\{\epsilon_j\}_{j=1}^{L_B}$ be the different energies with degeneracy g_j. For simplicity we consider the infinite temperature case, $\beta = 0$, i.e. $\chi(t) = \mathrm{tr}\left(e^{-itH}\right)$. If the set $\{\epsilon_j\}_{j=1}^{L_B}$ is independent and the degeneracies are generic, i.e. there exist a $q > 2$ such that*

$$\lim_{L \to \infty} S_q^{L_B} = 0, \quad \text{with} \quad S_q^{L_B} := \frac{\sum_{j=1}^{L_B} g_j^q}{\left(\sum_{j=1}^{L_B} g_j^2\right)^{q/2}}, \tag{18}$$

then for $L \to \infty$ the random variable $Y := \ln |\chi(t)|^2 / \sqrt{\sum_{j=1}^{L_B} g_j^2}$ converges in distribution to a Gaussian, more precisely

$$\frac{\log\left(|\chi(t)|^2\right)}{\sqrt{\sum_{j=1}^{L_B} g_j^2}} \to \mathsf{N}\left(0, \frac{\pi^2}{3}\right). \tag{19}$$

Alternatively $|\chi(t)|^{2/\sqrt{\sum_{j=1}^{L_B} g_j^2}} \to \mathsf{LogNormal}\left(0, \pi^2/3\right)$. Note that $\pi^2/3$ is the variance of $\mathsf{Unif}\,[0, 2\pi]$.

Remark. For $\beta \neq 0$ the result continues to hold provided Eq. (18) is satisfied. Namely Y still converges in distribution to $\mathsf{N}(0, \sigma)$ but we could not evaluate the variance σ (which now depends on β). However, as for the non-integrable case, we can anticipate that for sufficiently low temperature (large β) Eq. (18) will break down. The proof is yet another form of central limit theorem but in this case Y is a product of independent random variables, see Appendix F.

For completeness, we also give the expression for the moments in this case.

Theorem 6. *With the same setting and hypotheses as in theorem 5, one has*

$$\overline{|\chi(t)|^{2M}} = \prod_{j=1}^{L_B} \binom{2g_j M}{g_j M}. \tag{20}$$

	Quadratic	Bethe-Ansatz	Non-Integrable
Level spacing distribution	Poisson	Poisson	Wigner-Dyson
Normalized $\|\chi(t)\|^2$ distribution	LogNormal	Exp(1)	Exp(1)
Dimension of frontier	1.01 ± 0.12	1.24 ± 0.08	1.32 ± 0.08

Table I. Expectation of different metrics of chaos for increasingly more chaotic models (from left to right).

Consider for simplicity the non-degenerate case ($g_j = 1, L_B = L$). From Eq. (20) we obtain $\overline{|\chi(t)|^2} = 2^L = D$ which is the same result as for generic, non-integrable walkers. One may then be led to conjecture that quasi-free fractals are of the same size as non-integrable ones. However, analytically continuing Eq. (20) to $M = 1/2$ we obtain that the average distance of the quasi-free walker is $\overline{|\chi(t)|} = (4/\pi)^L = D^{0.348}$. This number is exponentially smaller in L than in the non-integrable case. In fact, from point iii) after Theorem 2 we get $\overline{|\chi(t)|} \simeq D^{1/2}\Gamma(3/2) = \sqrt{2}^L \sqrt{\pi}/2$. In other words, quasi-free fractals stay closer to the origin than non-integrable ones. This feature is also apparent in Fig. 1.

V. NUMERICS

We now come to the comparison of the previous theorems to realistic physical models for the case $\rho = e^{-\beta H}$. It is natural to expect that non-integrable systems have independent spectrum and that the weights are generic at infinite or sufficiently high temperature $1/\beta$. Instead, when the temperature is very low, the ground state $d_1 = e^{-\beta E_1} \text{tr}(\Pi_1)$ dominates and one can violate the CLT. On the other hand, quasi-free fermionic systems have only $L_B \leq L = O(\ln D)$ independent energies (the one-particle energies). So, for high temperature, looking at the distribution $|\chi(t)|^2$ we expect Exp(1) in the non-integrable case and LogNormal for quasi-free fermionic spectra. What about Bethe-Ansatz (BA) solvable models? One can make an argument for both cases. Indeed, say we consider the XXZ chain for concreteness. BA integrability implies that the spectrum (in each conserved sector) depends on $O(\ln D)$ quantities, the rapidities. However it is not clear if these quantities are combined to form the many body-spectrum in a way that does not introduces relations among the energies. We perform our numerics on the following XXZ chain next-to-nearest-neighbor coupling α

$$H = \sum_{j=1}^N \left(\sigma_j^x \sigma_{j+1}^x + \sigma_j^y \sigma_{j+1}^y + \Delta \sigma_j^z \sigma_{j+1}^z\right)$$
$$+ \alpha \sum_{j=1}^N \left(\sigma_j^x \sigma_{j+2}^x + \sigma_j^y \sigma_{j+2}^y + \Delta \sigma_j^z \sigma_{j+2}^z\right). \tag{21}$$

The model admits quasi free (for $\alpha = \Delta = 0$), Bethe-Ansatz ($\alpha = 0$), and non-integrable ($\alpha \neq 0$) phases. The model has several conserved quantities, and the pattern of degeneracies $d_j = \text{tr}(\Pi_j)$ is highly non-trivial, leading to d_j as high as 8 for a sensible fraction of j for $L = 10$. Our results confirm that, at infinite temperature, the distribution of the normalized $|\chi(t)|^2$ is Exp(1) in the non-integrable phase and LogNormal in the quasi-free one. We also observe an Exp(1) distribution for the BA case. Regarding the dimension of the fractal frontier we obtain $d_F = 1.32 \pm 0.08$ in the non-integrable XXZ model and $d_F = 1.01 \pm 0.12$ for the XX free spin chain. For the BA solvable XXZ model our simulations give $d_F = 1.24 \pm 0.08$. At this point we cannot claim for certain if the discrepancy from $4/3$ is due to the complexity of estimating the fractal frontier or genuinely $d_F \neq 4/3$ in the BA case. The latter scenario would mean that the number of relations among the energies for BA integrable models is not sufficient to violate the CLT for the random variable $|\chi(t)|^2$ but can be detected by looking at the frontier of the corresponding random walk. The results are summarized in Table I (see e.g. [43] for the first row).

VI. DISCUSSION AND CONCLUSIONS

When we are interested in understanding a quantum model, it is customary to consider functions of the model Hamiltonian H, which, depending on context, carry particular information on the problem at hand. One of the most versatile of such functions is $\text{tr}\, e^{-zH}$. When z is real, $\text{tr}\, e^{-zH}$ is the partition function and has information on the thermodynamics of the system. For complex $z = \beta + it$, its modulus square is known as the spectral form factor (SFF), and is important in a variety of fields

ranging from quantum chaos to black-hole dynamics. In this context, usually an average is performed further on the SFF over an ensemble of Hamiltonians. Typical examples are the (random) SYK model or the classical matrix ensembles such as GUE or GOE. Alternatively, in the spirit of statistical mechanics, where one observes the system for a sufficiently long time, one can average uniformly over time. It turns out that the two averages are related and using the latter, as already noted in [21], the SFF can be understood as a random walk.

In this paper, we push this analogy further. We generalize the SFF to $\chi(t) = \operatorname{tr} \rho e^{-itH}$ for any positive operator ρ, and we show how to associate any pair (ρ, H) with a random walk on the plane. For a Hamiltonian with spectral resolution $H = \sum_{j=1}^{N_B} E_j \Pi_j$ (E_j eigenenergies, Π_j spectral projectors, N_B number of blocks), at step n the walker rotates clockwise by an angle tE_n and steps forward by an amount $d_j = \operatorname{tr}(\rho \Pi_n)$. When t is a random variable uniformly distributed on the half-line, this is a random walk, i.e. a fractal, and we study the pair (ρ, H) through properties of this fractal geometry, in particular, we compute the Hausdorff dimension of its frontier. From this point of view, the moments of the SFF which correspond to the plateaus of [17] and have been studied extensively, correspond to moments of the distance of the walker from the origin at step N_B.

We show that, under two assumptions, the random walk becomes a Wiener process in the thermodynamic limit, for which the dimension of its frontier has been famously proved to be $d_F = 4/3$ using Schramm-Loewner evolutions methods [37]. The assumptions are i) that the energy levels are linearly independent over the set of rationals, and ii) a technical, Lyapunov-like condition. For $\rho = \mathbb{I}$ and non-degenerate spectra, the Lyapunov condition is automatically satisfied. Via numerical simulations, we show that, for $\rho = e^{-\beta H}$ and non-integrable H, the Lyapunov condition is satisfied at sufficiently high temperature $1/\beta$ (but notably fails at low temperature and in other documented cases). In these cases, we observe numerically that the dimension of the fractal frontier is approximately $d_F \simeq 4/3$, thus confirming the hypothesis of independence of the energy spectrum. The analogous result for the SFF is that the distribution of $|\chi(t)|^2$ properly normalized becomes $\mathsf{Exp(1)}$. This corresponds to $\overline{|\chi(t)|^{2m}} \simeq m! \left(\overline{|\chi(t)|^2} \right)^m$ a result widely known in the literature and sometimes called Gaussian approximation. Even if the hypothesis of independence of the energy levels can be proven, like in random matrix or SYK models, the Gaussian approximation hinges on the Lyapunov condition. This condition is violated at low temperature where only the lowest energy levels gets effectively populated[5]. On the other hand, we compute exactly the moments of the SFF without the Gaussian approximation solving the classical problem of a random walker taking steps of unequal lengths. The results agree with numerical experiments on the SYK model.

For free, integrable models, the condition of independent spectrum fails spectacularly as the number of independent energies is at most N where N is the number of free modes, in spite of a Hilbert space dimension D exponential in N. This means that there are at least $D - N$ relations among the energies of the form $\sum_{j=1}^{D} a_j E_j = 0$ with $a_j \in \mathbb{Z}$. In this case, even when the Lyapunov condition is satisfied, the random walk is no longer a sum of independent variables. The exponentially many relations among the energies imply a correlation among a large fraction of the random variables that are no longer independent. As a result, the central limit theorem breaks down, and the random walk is not a Wiener process in the thermodynamic limit. Summarizing, when the Lyapunov conditions are satisfied, a value for the dimension of the fractal frontier close to $4/3$ signals that the random variables that form the random walk are sufficiently independent, while a value away from $4/3$ signals the breakdown of the central limit theorem and dependent variables. This result provides a novel method to inquire the difficult problem of independence of random variables. For instance, a long standing problem is that of the Bethe-Ansatz (BA) solvable case. The study of the BA fractal shows that is likely to be smaller than $4/3$ and therefore consistent with a breakdown of the CLT and a novel, universal value, but this analysis requires further investigation.

There are several directions that opens up for future studies. On the one hand, one can consider other kind of quantum mechanical objects, such as entanglement Hamiltonians (obtained as minus the logarithm of a partial trace of a quantum state), quantum states themselves, or more general evolutions which include decoherence and dissipation. The study of the interplay between the SFF and the operator entanglement spectrum [44] is indeed particularly promising. Additionally, other properties of fractals can be used or even fractals embedded in a larger dimensional space. One intriguing possibility is to study a particular class of quantum many-body Hamiltonians whose eigenstates can be characterized as doped stabilizer states [45]. The doping refers to a very gentle way of perturbing otherwise integrable Hamiltonians. These Hamiltonians, although non-integrable, feature classical algorithms efficient in computing their time evolution, thermal states, and low-energy eigenstates. The study of their SFF and the associated fractal can thus shed some light in the direction of understanding how integrable features may be not immediately lost and give insight towards a quantum KAM theorem, sewing together the chaotic features of the spectrum and those of the eigenvectors of a Hamiltonian [46].

---

[5] To be precise, this feature is stable as the size approaches the thermodynamic limit for models with a gap above the ground state. For models with gapless excitations this feature appears in a crossover region for finite size

ACKNOWLEDGMENTS

Appendix A: Proof of Theorem 1

We consider a random Hamiltonian $H(x) = \sum_{j=1}^{N_B} E_j(x)\Pi_j(x)$ where x is the collection of (static) random variables. By assumption d_j do not depend on x. Starting from $\chi_x(t) = \sum_{j=1}^{N_B} d_j e^{-itE_j(x)}$, for any realization x, we get

$$|\chi_x(t)|^2 = \sum_{i,j=1}^{N_B} F_{i,j} e^{-it(E_i(x)-E_j(x))} \tag{A1}$$

having defined, for convenience, $F_{i,j} = d_i d_j$. Hence

$$I_m := |\chi_x(t)|^{2m} = \sum_{i_1 \cdots i_m} \sum_{j_1 \cdots j_m} F_{i_1,j_1} \cdots F_{i_m,j_m} \times$$
$$\times \exp\left(-it \sum_{l=1}^{m} (E_{i_l}(x) - E_{j_l}(x))\right) \tag{A2}$$

which we write compactly as

$$|\chi_x(t)|^{2m} = \sum_{s,r} f(s,r) e^{-it(\boldsymbol{E}_s(x)-\boldsymbol{E}_r(x))} \tag{A3}$$

having defined the multi indices $s = (s_1, \ldots, s_m)$ corresponding to $\boldsymbol{E}_s(x) = E_{s_1}(x) + E_{s_2}(x) + \cdots E_{s_m}(x)$ and similarly for r and $\boldsymbol{E}_r(x)$ together with the coefficients $f(s,r)$. Note that, if the degeneracies $\operatorname{tr} \Pi_j(x)$ do not depend on x, the sequences $\{s_j\}$ depend only on N_B and not on x. It is useful to go to the occupation number representation. For any sequence $\{s_i\}_{i=1}^{m}$ we define the (bosonic) occupation numbers:

$$n_k^s := \sum_{i=1}^{m} \delta_{E_k(x),E_{s_i}(x)}, \tag{A4}$$

so n_k^s counts how many terms in $\{E_{s_i}(x)\}_{i=1}^{M}$ have energy $E_k(x)$. We also define $\boldsymbol{n}^s = \left(n_1^s, \ldots, n_{N_B}^s\right)$ and write

$$\boldsymbol{E}_s(x) = \sum_{k=1}^{N_B} n_k^s E_k(x) = \boldsymbol{n}^s \cdot \boldsymbol{E}(x). \tag{A5}$$

Taking the infinite time average we get $\overline{e^{-it(\boldsymbol{E}_s(x)-\boldsymbol{E}_r(x))}} = \delta_{(\boldsymbol{E}(x)\cdot(\boldsymbol{n}^s-\boldsymbol{n}^r))}$ where δ_X is a Kronecker delta. If the distribution of the eigenvalues $\boldsymbol{E}$ is absolutely continuous the set $\{E(x)\}_{k=1}^{N_B}$ is rationally independent almost everywhere. So, for almost any x, $\delta_{(\boldsymbol{E}(x)\cdot(\boldsymbol{n}^s-\boldsymbol{n}^r))} = \delta_{(\boldsymbol{n}^s-\boldsymbol{n}^r)}$. So we obtain

$$\overline{|\chi_x(t)|^{2m}} = \sum_{s,r} f(s,r)\delta_{(\boldsymbol{n}^s-\boldsymbol{n}^r)}. \tag{A6}$$

Incidentally the above equation does not depend on x anymore and so we obtain also $\overline{|\chi_x(t)|^{2m}} = \mathsf{E}_x\left[\overline{|\chi_x(t)|^{2m}}\right]$. We now take the average over x of Eq. (A3):

$$\mathsf{E}_x\left[|\chi_x(t)|^{2m}\right] = \sum_{s,r} f(s,r)\mathsf{E}_x\left[e^{-it(\boldsymbol{E}(x)\cdot(\boldsymbol{n}^s-\boldsymbol{n}^r))}\right]$$

$$= \sum_{s,r} f(s,r)\delta_{(\boldsymbol{n}^s-\boldsymbol{n}^r)}$$

$$+ \sum_{s,r} f(s,r)\mathsf{E}_x\left[e^{-it(\boldsymbol{E}(x)\cdot(\boldsymbol{n}^s-\boldsymbol{n}^r))}\right]\delta_{(\boldsymbol{n}^s\neq\boldsymbol{n}^r)}. \tag{A7}$$

Let us call $O(t)$ the last term above. If the distribution of $\boldsymbol{E}$ is absolutely continuous: $\mu(d\boldsymbol{E}) = P_{\boldsymbol{E}}(\boldsymbol{E})d\boldsymbol{E}$, $\mathsf{E}_x\left[e^{-it(\boldsymbol{E}(x)\cdot(\boldsymbol{n}^s-\boldsymbol{n}^r))}\right] = \hat{P}_{\boldsymbol{E}}(t(\boldsymbol{n}^s-\boldsymbol{n}^r))$ is the Fourier transform of a function in L^1. By Riemann-Lebesgue lemma $\lim_{t\to\infty}\hat{P}_{\boldsymbol{E}}(t(\boldsymbol{n}^s-\boldsymbol{n}^r)) = 0$ whenever $\boldsymbol{n}^s \neq \boldsymbol{n}^r$. So we get $\lim_{t\to\infty} O(t) = 0$ which implies that $\overline{O(t)} = 0$ which proves the claim.

Appendix B: Proof of Theorem 2

The setting is very similar as for the Lyapunov central limit theorem, which concerns the sum of independent variables with different distributions. However, the variance of each variables, d_j^2, may depend also n, which prevents direct application of Lyapunov theorem. The dependence on n introduces a sort of correlation between the different variables. As we shall see, it turns out that in our case the Lyapunov condition is still both necessary and sufficient for the Gaussiantity of the normalized sum as $n \to \infty$. Let us compute the characteristic function of the random variable $Y_n = Z_n/\Delta Z_n$ ($\boldsymbol{k} = (k_1, k_2)$):

$$\overline{e^{i\boldsymbol{k}Y_n}} = \exp\left(i\sum_{j=1}^n \frac{d_j}{\Delta Z_n}(k_1\cos(tE_j) + k_2\sin(tE_j))\right). \tag{B1}$$

Under assumption of independence of the energies E_j the time average becomes the uniform average over the torus $\mathbb{T}^n$ and we obtain

$$\overline{e^{i\boldsymbol{k}Y_n}} = \prod_{j=1}^n \int \frac{d\vartheta_j}{2\pi}\exp\left(i\frac{d_j}{\Delta Z_n}(k_1\cos(\vartheta_j) + k_2\sin(\vartheta_j))\right)$$

$$= \prod_{j=1}^n J_0\left(\frac{d_j}{\Delta Z_n}\|\boldsymbol{k}\|\right)$$

where J_0 is the Bessel function of the first kind, analytic in a neighborhood of zero. Let us define $\ln J_0(x) = \sum_{p=1}^\infty b_p x^{2p}$ (for x small enough $J_0(x) > 0$). Note that $b_1 = -1/4$. Then

$$\overline{e^{i\boldsymbol{k}Y_n}} = \exp\left(\sum_{j=1}^n\sum_{p=1}^\infty b_p\left(\frac{d_j}{\Delta Z_n}\right)^{2p}\|\boldsymbol{k}\|^{2p}\right). \tag{B2}$$

Defining $R_p^n = \sum_{j=1}^n (d_j/\Delta Z_n)^{2p}$ the above is written as

$$\overline{e^{i\boldsymbol{k}Y_n}} = \exp\left(\sum_{p=1}^\infty b_p R_p^n\|\boldsymbol{k}\|^{2p}\right). \tag{B3}$$

The Lyapunov condition states that there is a $q > 1$ such that $R_q^n \to 0$ as $n \to \infty$. We will show that the Lyapunov condition implies that $R_p^n \to 0$ for all $p > 1$. First note that $\lim_{n\to\infty} R_q^n = 0$ iff

$$\lim_{n\to\infty} \frac{\|\boldsymbol{d}_n\|_{2q}}{\|\boldsymbol{d}_n\|_2} = 0 \tag{B4}$$

where $\|\boldsymbol{x}\|_p = \left(\sum_{j=1}^n |x_j|^p\right)^{1/p}$ and $\boldsymbol{d}_n = (d_1, d_2, \ldots, d_n)$. Now for $p \geq 2q$ $\|\boldsymbol{x}\|_p \leq \|\boldsymbol{x}\|_{2q}$ so Eq. (B4) implies $R_p^n \to 0$ for all $p > 2q$. Consider now $p \in (2, 2q)$ and define $\boldsymbol{x}_n = \boldsymbol{d}_n/\|\boldsymbol{d}_n\|_2$ so that $\|\boldsymbol{x}_n\|_2 = 1$. For all $r \in (0,1)$ define

$x^r := (|x(1)|^r, \ldots, |x(n)|^r)$. Then

$$\|x^r\|_{2/r} = (\|x\|_2)^r$$

$$\|x^{1-r}\|_{2q/(1-r)} = \left(\|x\|_{2q}\right)^{1-r}.$$

By Hölder inequality, for all $p \in (2, 2q)$,

$$\|x\|_p \leq \|x^r\|_{2/r} \|x^{1-r}\|_{2q/(1-r)} \tag{B5}$$

as long as

$$\frac{1}{p} = \frac{r}{2} + \frac{1-r}{2q} \tag{B6}$$

which implies $r = (2q - p)/(p(q-1))$. This is indeed in $(0,1)$ for $p \in (2, 2q)$. Applying Eq. (B5) to our sequence of sequences x_n we get

$$\|x_n\|_p \leq \left(\|x_n\|_{2q}\right)^{1-r} \tag{B7}$$

which implies $\|x_n\|_p \to 0$ also for $p \in (2, 2q)$. Hence we obtain that $R_p^n \to 0$ for all $p > 1$ as claimed, i.e. $\lim_{n\to\infty} R_p^n = \delta_{p,1}$. To pass the limit inside the series in Eq. (B3) note that $R_q^n \leq 1$ for all q so $\left|b_p R_p^n \|k\|^{2p}\right| \leq |b_p| \|k\|^{2p} =: M_p$ and $\sum_p M_p = |\ln J_0(\|k\|)| < \infty$ and by Tannery's theorem we can exchange the limit with the series and obtain

$$\lim_{n\to\infty} \overline{e^{ikY_n}} = e^{-\|k\|^2/4}. \tag{B8}$$

Fourier transforming we get for the probability distribution of $Y = \lim_{n\to\infty} Y_n$

$$P_Y(y) = \int_{\mathbb{R}^2} \frac{dk}{(2\pi)^2} e^{ik \cdot x} e^{-\|k\|^2/4} \tag{B9}$$

$$= \frac{1}{\pi} e^{-\|y\|^2}. \tag{B10}$$

The converse statement also trivially holds, i.e. if Eq. (B4) is not satisfied for any $q > 1$ the cumulants of Y are all non-zero and its distribution is not Gaussian.

Given the joint distribution $P_Y(y)$ it is straightforward to obtain the distribution of the distance square from the origin $P_{|Y|^2}(r)$:

$$P_{|Y|^2}(r) = \int_{\mathbb{R}^2} dy\, \delta(r - \|y\|^2) P_Y(y)$$

$$= 2\pi \int_0^\infty \rho\, d\rho\, \delta(r - \rho^2) \frac{1}{\pi} e^{-\|y\|^2}$$

$$= \vartheta(r) e^{-r}.$$

Analogously one obtains $P_{|Y|}(u) = \vartheta(u) 2u e^{-u^2}$. Going back to the unnormalized variables one obtains approximately $P_{|Z_n|^2}(v) \simeq \vartheta(\nu) \exp\left(-\nu/\Delta Z_n^2\right)/\Delta Z_n^2$.

Note that the distribution of $|Z_n|^2$ can be written exactly under the assumption of independent spectrum [6]. Following [6] (see Eq. (F2))

$$\text{Prob}\left(|Z_n|^2 < r^2\right) = \int_0^\infty d\rho\, r J_1(r\rho) \prod_{j=1}^n J_0(d_j\rho). \tag{B11}$$

Substituting $r^2 = s$ and differentiating with respect to s we obtain

$$P_{|Z_n|^2}(r) = \frac{1}{2} \int_0^\infty d\rho\, \rho J_0(\sqrt{s}\rho) \prod_{j=1}^n J_0(d_j\rho), \tag{B12}$$

which is Eq. (F3) of [6] after simplification.

Appendix C: Convergence to the Wiener process

Here we show that under certain conditions the random walk defined by Eq. (10) converges to a Wiener process. The steps are similar to those of Section B. As mentioned in the main text, if the energies are independent, the path has independent increment. Let us compute the probability distribution of the following random variable

$$\Delta^N(s,h) := W_{s+h}^N - W_s^N = \frac{1}{\Delta Z_N} \sum_{j=\lfloor Ns \rfloor+1}^{\lfloor N(s+h) \rfloor} d_j e^{-itE_j}, \tag{C1}$$

where t is a random variable subject to infinite-time average. Under assumption of independence of the energies its characteristic function is

$$\overline{e^{i\boldsymbol{k}\Delta^N(s,h)}} = \prod_{j=\lfloor Ns \rfloor+1}^{\lfloor N(s+h) \rfloor} J_0\left(\frac{d_j}{\Delta Z_N}\|\boldsymbol{k}\|\right). \tag{C2}$$

Let us, as in Section B, write $\ln J_0(x) = \sum_{q=1}^{\infty} b_q x^{2q}$. Then

$$\overline{e^{i\boldsymbol{k}\Delta^N(s,h)}} = \exp\left(\sum_{q=1}^{\infty} \sum_{j=\lfloor Ns \rfloor+1}^{\lfloor N(s+h) \rfloor} \|\boldsymbol{k}\|^{2q} b_q \left(\frac{d_j}{\Delta Z_N}\right)^{2q}\right). \tag{C3}$$

Define

$$R_q^N(h,s) := \frac{\sum_{k=\lfloor Ns \rfloor+1}^{\lfloor N(s+h) \rfloor} d_k^{2q}}{\left(\sum_{k=1}^{N} d_k^2\right)^q}. \tag{C4}$$

We now observe that $R_q^N(h,s) \leq R_q^N$ for all allowed s, h and all $q > 1$. Hence, the assumption that the weights are generic implies that

$$\lim_{N\to\infty} R_q^N(h,s) = 0, \text{ for } q > 1. \tag{C5}$$

Using Eq. (12) and repeating the steps in Section B to pass the limit inside the exponential we obtain (remind that $b_1 = -1/4$)

$$\lim_{N\to\infty} \overline{e^{i\boldsymbol{k}\Delta^N(s,h)}} = e^{-h\|\boldsymbol{k}\|^2/4}. \tag{C6}$$

Fourier transforming, we obtain the distribution of the random variable $\Delta^N(s,t)$ in the limit $N \to \infty$:

$$W_{s+h}^N - W_s^N \xrightarrow{d} \frac{1}{h\pi} e^{-\|\boldsymbol{x}\|^2/h}. \tag{C7}$$

Then we obtain

$$\text{Prob}\left(W : |W_{s+h} - W_s| \leq \rho\right) = \frac{2\pi}{h\pi} \int_0^{\rho} dr\, re^{-r^4/h}. \tag{C8}$$

redefining times such that $s = 2s'$ we obtain Eq. (11) of the main text, hence $W_{s'}^N$ converges to a Wiener process.

Appendix D: Non-degeneracy and independence

To compute the moments of the SFF in the literature one often finds a non-degeneracy condition. Here we show what is the relation between non-degeneracy and linear independence over the rationals. First we need the following definition:

Definition 1. We say that the the numbers $\{E_k\}_{k=1}^{D}$, assumed to be all different, satisfy the non-degeneracy condition at order $M \in \mathbb{N}$ (M-ND) if, for any pair of sequences $\alpha_i, \beta_i \in \{1, 2, \ldots, D\}$, $i = 1, 2, \ldots, M$, the equation

$$\sum_{j=1}^{M} E_{\alpha_j} = \sum_{j=1}^{M} E_{\beta_j} \tag{D1}$$

implies that $\{\alpha_1, \alpha_2, \ldots, \alpha_M\}$ is a permutation of $\{\beta_1, \beta_2, \ldots, \beta_M\}$, i.e. there exist a permutation $\pi \in \mathbb{S}_M$ such that $\alpha_i = \beta_{\pi(i)}$.

Note that M-ND implies N-ND for all $1 \leq N \leq M$. It is useful to go to the occupation number representation. For any $\{\alpha_i\}_{i=1}^M$ we define the (bosonic) occupation numbers:

$$n_k^\alpha := \sum_{i=1}^M \delta_{E_k, E_{\alpha_i}}, \tag{D2}$$

so n_k^α counts how many terms in $\{E_{\alpha_i}\}_{i=1}^M$ have energy E_k. Note that the occupation number representation is unique modulo permutations, i.e. $n_k^\alpha = n_k^\beta, \forall k \iff \alpha = \pi(\beta)$ for some permutation π. Moreover, clearly,

$$\sum_{j=1}^M E_{\alpha_j} = \sum_{k=1}^D n_k^\alpha E_k. \tag{D3}$$

We have the following result:

Lemma. *The numbers $\{E_n\}_{n=1}^D$ satisfy non-degeneracy at order M $\forall M \in \mathbb{N}$ (ℕND) if and only if the energies $\{E_n\}_{n=1}^D$ are linearly independent over the rationals.*

Proof. First, the $\Leftarrow$ direction. Consider two sequences α_i, β_i. Using the mapping Eq. (D2), M-ND Eq. ((D1)) can be written as

$$\sum_{k=1}^D \left(n_k^\alpha - n_k^\beta\right) E_k = 0. \tag{D4}$$

Now independence implies that $n_k^\alpha = n_k^\beta$ and for what we have said this implies $\alpha = \pi(\beta)$ for some permutation π. The statement holds for all possible M so this direction is proven. For the $\Rightarrow$ direction, consider the equation for linear independence:

$$\sum_{k=1}^D m_k E_k = 0, \tag{D5}$$

with $m_k \in \mathbb{Z}$ for $k = 1, \ldots, D$. We can always find sequences α, β such that $m_k = n_k^\alpha - n_k^\beta$. For example, for $k = 1, \ldots, D$, if $m_k > 0$ we can choose $n_k^\alpha = m_k$ and $n_k^\beta = 0$ and conversely if $m_k < 0$ we can choose $n_k^\beta = |m_k|$ and $n_k^\alpha = 0$. By M-ND (for some M) this implies $m_k = n_k^\alpha - n_k^\beta = 0$, i.e. independence. $\qquad\square$

Appendix E: Moments of the spectral form factor

In this section, we give the exact form of the infinite time moments of the spectral form factor assuming that the energies $\{E_j\}_{j=1}^{N_B}$ satisfy nondegeneracy at order m. We recall from Sec. A

$$I_m := |\chi(t)|^{2m} = \sum_{i_1 \cdots i_m} \sum_{j_1 \cdots j_m} F_{i_1, j_1} \cdots F_{i_m, j_m} \times$$
$$\times \exp\left(-it \sum_{l=1}^m \left(E_{i_l} - E_{j_l}\right)\right) \tag{E1}$$

which we write compactly as

$$|\chi(t)|^{2m} = \sum_{s,r} f(s,r) e^{-it(\boldsymbol{E}_s - \boldsymbol{E}_r)} \tag{E2}$$

with multi indices $s = (s_1, \ldots, s_m)$ corresponding to $\boldsymbol{E}_s = E_{s_1} + E_{s_2} + \cdots E_{s_m}$ and similarly for r and $\boldsymbol{E}_r$ together with the coefficients $f(s,r)$. Taking the infinite-time average we get $\overline{e^{-it(\boldsymbol{E}_s - \boldsymbol{E}_r)}} = \delta\left(\boldsymbol{E}_s - \boldsymbol{E}_r\right)$. If the energies satisfy m order non-degeneracy, the only way to fulfill the constraint $\delta\left(\boldsymbol{E}_s - \boldsymbol{E}_r\right)$ is that the string r is a permutation of s. There are multiplicities, however, that have to be accounted for. The result is

$$\overline{|\chi(t)|^{2m}} = \sum_{s,r} f(s,r) \delta\left(\boldsymbol{E}_s - \boldsymbol{E}_r\right) \tag{E3}$$

$$= \sum_s \sum_{\pi \in \mathbb{S}_m} f(s, \pi(s)) \frac{1}{c(s)} \tag{E4}$$

the multiplicity $c(s)$ is the number of different permutations of s given that some member of $\boldsymbol{E}_s$ might be equal. Having defined, for any string $\{s_i\}_{i=1}^m$ and $k = 1, \ldots, N_B$, the occupation number $n_k^s = \sum_{i=1}^m \delta_{E_k, E_{s_i}}$ which counts how many energies E_k are in $\boldsymbol{E}_s$, clearly one has $\sum_{i=1}^{N_B} n_i^s = m$. Then the multiplicity factor is given by

$$c(s) = \prod_{i=1}^{N_B} n_i^s! \tag{E5}$$

Now, starting from

$$\overline{|\chi(t)|^{2m}} = \sum_{s_1, \ldots, s_m} c(s)^{-1} \sum_{\pi \in \mathbb{S}_m} F_{s_1, \pi(s_1)} \cdots F_{s_m, \pi(s_m)}, \tag{E6}$$

we use $F_{i,j} = d_i d_j$ so $f(s, \pi(s)) = \prod_{i=1}^{N_B} d_i^{2n_i^s}$ and is independent of π. Then

$$\overline{|\chi(t)|^{2m}} = \sum_s \frac{1}{\prod_i n_i!} \sum_\pi \prod_{i=1}^{N_B} d_i^{2n_i^s} \tag{E7}$$

$$= \sum_s \frac{m!}{\prod_i n_i!} \prod_{i=1}^{N_B} d_i^{2n_i^s} \tag{E8}$$

$$= \sum_{\sum_i k_i = k} \left[\frac{m!}{\prod_i n_i!} \right]^2 \prod_{i=1}^{N_B} d_i^{2n_i} \tag{E9}$$

where the last line comes from the multinomial formula that allows to go from index labels $s = (s_1, \ldots, s_k)$ to occupation number labels n_i, $i = 1, \ldots, N_B$. Finally the m-th moment of the spectral form factor is given by

$$\overline{|\chi(t)|^{2m}} = (m!)^2 \sum_{\sum_i n_i = m} \prod_{i=1}^{N_B} \left(\frac{d_i^{n_i}}{n_i!} \right)^2 \tag{E10}$$

$$= \sum_{\sum_i n_i = m} \left(\begin{matrix} m \\ n_1, \cdots, n_{N_B} \end{matrix} \right)^2 \prod_{i=1}^{N_B} d_i^{2n_i}, \tag{E11}$$

where in the last line we introduced the multinomial coefficient. In case $d_j = 1$ for all j the above reduces to the expression found in [31]. Equation (E10), although exact, is difficult to manage. For example, it is not clear how to estimate the order of magnitude or the leading contribution to the moments. In order to obtain a more manageable expression let us define the following generating function

$$B(z) := \sum_{k=0}^\infty \frac{I_k}{(k!)^2} z^k \tag{E12}$$

$$= \overline{I_0 \left(2 |\chi(t)| \sqrt{z} \right)}, \tag{E13}$$

where I_0 is the modified Bessel function of the first kind. The above sum can be obtain in closed form, indeed,

$$B(z) = \sum_{k=0}^\infty \sum_{\sum_i k_i = k} \prod_{i=1}^{N_B} \frac{\left(d_i^2 z \right)^{k_i}}{(k_i!)^2} \tag{E14}$$

$$= \prod_{i=1}^{N_B} \sum_{n=0}^\infty \frac{\left(d_i^2 z \right)^n}{(n!)^2}. \tag{E15}$$

The last sum is again I_0, more precisely

$$B(z) = \prod_{i=1}^{N_B} I_0 \left(2 d_i \sqrt{z} \right), \tag{E16}$$

In principle one can obtain the moments via

$$I_m = m! \left. \frac{d^m B}{dz^m} \right|_{z=0},$$

(E17)

but we are proposing a better expression momentarily.

For convenience we define $I(x) = I_0(2\sqrt{x})$, and the coefficients a_n via the following series ($I(x) \geq 1$ for $x \geq 0$ so the logarithm is well defined and analytic in a neighborhood of zero)

$$\ln I(x) = \sum_{n=0}^{\infty} a_n \frac{x^n}{n!}.$$

(E18)

then

$$
\begin{aligned}
\ln(B(z)) &= \sum_{i=1}^{N_B} \ln I\left(d_i^2 z\right) \\
&= \sum_{i=1}^{N_B} \sum_{n=0}^{\infty} a_n d_i^{2n} \frac{z^n}{n!} \\
&= \sum_{n=0}^{\infty} a_n X_n \frac{z^n}{n!},
\end{aligned}
$$

(E19)

where we defined $X_n = \sum_{i=1}^{N_B} d_i^{2n}$. The coefficients a_n are the cumulants of a random variable with moments $\mu_k = 1/k!$. So $a_1 = 1$, $a_2 = 1/2 - 1^2 = -1/2$, $a_3 = \ldots = 2/3$ and so on. Hence the moments $I_k/k!$ have cumulants $a_n X_n$. We can then use the standard recursion between moments and cumulants:

$$\frac{I_p}{p!} = \sum_{q=1}^{p-1} \binom{p-1}{q-1} a_q X_q \frac{I_{p-q}}{(p-q)!} + a_p X_p.$$

(E20)

which is Eq. (15) from the main text. With this recursion one easily obtains Eqns. (16-17) of the main text and also, for example, assuming 5-ND,

$$
\begin{aligned}
I_4 &= 24\left(X_1\right)^4 - 72\left(X_1\right)^2 X_2 + 18\left(X_2\right)^2 \\
&\quad + 64 X_1 X_3 - 33 X_4
\end{aligned}
$$

(E21)

$$
\begin{aligned}
I_5 &= 120\left(X_1\right)^5 - 600 X_2 \left(X_1\right)^3 + 800 X_3 \left(X_1\right)^2 \\
&\quad + 450\left(X_2\right)^2 X_1 - 825 X_4 X_1 \\
&\quad - 400 X_2 X_3 + 456 X_5.
\end{aligned}
$$

(E22)

Appendix F: Limit distribution for free fermionic spectra

Consider H with spectrum $E_{\boldsymbol{n}} = \sum_{k=1}^{L} n_k \Lambda_k + E_0$ with $n_k = 0, 1$. We first compute ($z = \beta + it$)

$$
\begin{aligned}
\mathrm{tr}\left(e^{-zH}\right) &= e^{-zE_0} \sum_{\{n_k\}} \exp\left(-z \sum_{k=1}^{L} n_k \Lambda_k\right) \\
&= e^{-zE_0} \sum_{\{n_k\}} e^{-zn_1\Lambda_1} \cdots e^{-zn_L\Lambda_L} \\
&= e^{-zE_0} \prod_{k=1}^{L} \left(1 + e^{-z\Lambda_k}\right).
\end{aligned}
$$

From here on we stick to infinite temperature i.e. $z = it$. If some levels are degenerate we get

$$\left|\mathrm{tr}\left(e^{-itH}\right)\right|^2 = \prod_{j=1}^{L_B} \left|1 + e^{-it\epsilon_j}\right|^{2g_j}$$

$$= \prod_{j=1}^{L_B} \left(2\cos\left(t\epsilon_j/2\right)\right)^{2g_j}. \tag{F1}$$

Assuming that the levels $\{\epsilon_j\}_{j=1}^{L_B}$ are independent implies that (upon considering t a random variable) $\left|\mathrm{tr}\left(e^{-itH}\right)\right|^2$ is a product of independent random variables Y_j. So the logarithm of the product is a sum of independent random variables $\ln Y_j$. The moment generating function of $\ln Y_j$ is

$$\overline{(Y_j)^\lambda} = \int_0^{2\pi} \frac{d\vartheta}{2\pi} \left(2\cos\left(\vartheta\right)\right)^{2g_j\lambda} = \frac{4^{\lambda g_j}\Gamma\left(\frac{1}{2} + \lambda g_j\right)}{\sqrt{\pi}\Gamma\left(1 + \lambda g_j\right)} \tag{F2}$$

$$= G(\lambda g_j) = \exp\left[\sum_{n=2}^{\infty} c_n \left(g_j\lambda\right)^n\right], \tag{F3}$$

where in the last equation we defined the function G and the coefficients c_n (since the function in (F2) is analytic and positive for $\lambda > -1/2$ its logarithm is analytic in the same region). Explicitly $c_2 = \pi^2/6$.

Let us define the following random variable

$$Q^L = \frac{\ln|\chi(t)|^2}{\sqrt{\sum_{j=1}^{L_B} g_j^2}}, \tag{F4}$$

and the ratios

$$S_p^{L_B} = \frac{\sum_{j=1}^{L_B} (g_j)^2}{\left(\sum_{j=1}^{L_B} g_j^2\right)^{p/2}}. \tag{F5}$$

By the same arguments as in Section B the assumption that the one-particle degeneracies g_j are generic implies that

$$\lim_{L\to\infty} S_p^L = 0, \ \forall p > 2. \tag{F6}$$

The random variable Q^L has the following characteristic function

$$\overline{e^{ikQ^L}} = \exp \sum_{j=1}^{L_B} \sum_{p=2}^{\infty} c_p S_p^{L_B} \left(ik\right)^p. \tag{F7}$$

To show that we can pass the limit inside the exponential note that $\left|S_p^{L_B}\right| \leq 1$ for all p and since $\ln(G(\lambda))$ is analytic, the coefficients are bounded by $|c_p| \leq C^{p+1}$ for some constant C and $\sum_{p=2}^{\infty} C^{p+1}|k|^p < \infty$ for $|k|$ small enough so that the limit and the sum can be swapped by Tannery's theorem. Finally, we obtain, in the thermodynamic limit,

$$\lim_{L\to\infty} \overline{e^{i\lambda Q^L}} = e^{-(\pi^2/6)\lambda^2}. \tag{F8}$$

After Fourier transform, we get

$$\frac{\ln|\chi(t)|^2}{\sqrt{\sum_{j=1}^{L_B} g_j^2}} \xrightarrow{d} \mathsf{N}\left(0, \frac{\pi^2}{3}\right). \tag{F9}$$

For finite temperature, $\beta \neq 0$, the steps are the same, but we could not evaluate the variance in closed form, which now depends on β.

Appendix G: Moments for free fermionic spectra

Here we want to compute $I_M = \overline{|\chi(t)|^{2M}}$ when H has the free Fermionic spectrum, under the assumption that the $\{\epsilon_j\}_{j=1}^{L_B}$ are independent. Following the previous section we have

$$|\chi(t)|^{2M} = \prod_{j=1}^{L_B} \left(e^{it\epsilon_j/2} + e^{-it\epsilon_j/2} \right)^{2g_j M}$$

$$= \prod_{j=1}^{L_B} \sum_{k=0}^{2g_j M} \binom{2g_j M}{k} e^{-it\epsilon_j(g_j M - k)}$$

$$= \sum_{k_1=0}^{2g_j M} \cdots \sum_{k_{L_B}=0}^{2g_j M} \binom{2g_j M}{k_1} \cdots \binom{2g_j M}{k_{L_B}} \times$$

$$\times \exp\left(-it \sum_{j=1}^{L_B} \epsilon_j(g_j M - k_j) \right).$$

Taking the infinite time average independence of the ϵ_j implies that only the terms with $k_j = g_j M$ remain and we get

$$\overline{|\chi(t)|^{2M}} = \prod_{j=1}^{L_B} \binom{2g_j M}{g_j M}. \tag{G1}$$

Appendix H: Numerics on physical models

1. Check of the Lyapunov condition in Eq.(7) at high temperature

We show that at infinite temperature $T \to \infty$ (with $\beta = 1/T$) implying $\rho = \mathbb{I}$, in case of physical models (local Hamiltonians), with spectral resolution $H = \sum_{j=1}^{N_B} E_j \Pi_j$, the weights $d_j = \text{tr}(\Pi_j)$, satisfy the Lyapunov condition Eq. (7), i.e. are *generic*. For a given D-dimensional Hamiltonian, we define

$$R_q^n = \frac{\sum_{j=1}^{n} d_j^{2q}}{\left(\sum_{j=1}^{n} d_j^2 \right)^q}, \tag{H1}$$

where $n \in \{1, 2, \ldots .N_B\}$. We investigate this behavior using the following XXZ Hamiltonian with next-to-nearest-neighbor (NNN) interactions (Eq. (21) of the main text) with periodic boundary conditions, $\sigma_{N+j}^{\alpha} = \sigma_j^{\alpha}$:

$$H = \sum_{j=1}^{N} \left(\sigma_j^x \sigma_{j+1}^x + \sigma_j^y \sigma_{j+1}^y + \Delta \sigma_j^z \sigma_{j+1}^z \right)$$

$$+ \alpha \sum_{j=1}^{N} \left(\sigma_j^x \sigma_{j+2}^x + \sigma_j^y \sigma_{j+2}^y + \Delta \sigma_j^z \sigma_{j+2}^z \right). \tag{H2}$$

This model interpolates between three regimes:

- *non-integrable* case ($\alpha \neq 0$),

- *Bethe Ansatz (BA) integrable* case ($\alpha = 0$),

- *quadratic quasi-free integrable* case ($\Delta = 0$, $\alpha = 0$).

We numerically diagonalize the Hamiltonian for finite system sizes N and identify eigenvalue degeneracies using a numerical threshold of $\epsilon = 10^{-8}$.

In Fig. 2, we present numerical evidence that the weights d_j behave generically in both the integrable (Bethe Ansatz) and non-integrable regimes, i.e. the ratio decays exponentially with the system size N (upper panels), and as a power-law with the eigenvalue index n (lower panels). Note that, as shown in the proof of Theorem 2, if, for $M \to \infty$, $R_q^M \to 0$ for a certain value of $q > 1$, then $R_q^M \to 0$ for all $q > 1$, and so it is sufficient to check the statement for a single q.
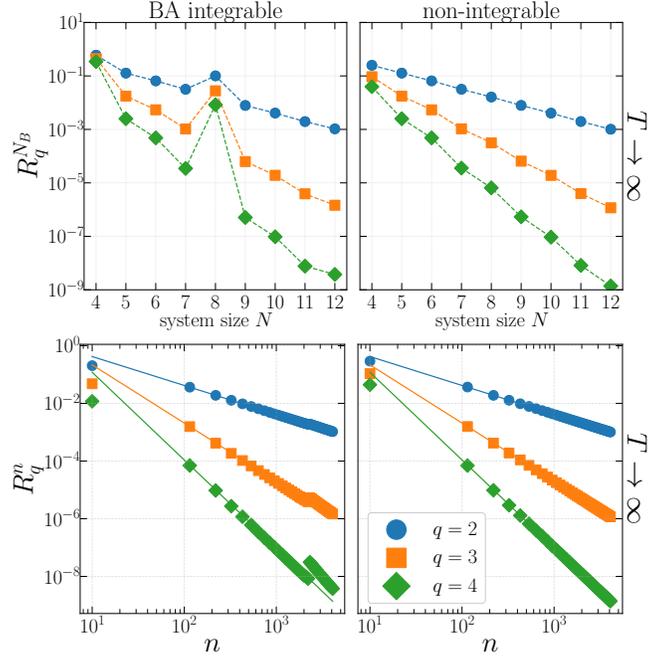
Figure 2. Numerical check of (7) for the paradigmatic example of a physical (local) Hamiltonian given by XXX+NNN chain in (21) at high temperature. *Upper panels*: Decay of the ratios $R_q^{N_B}$ for various system sizes N, where N_B denotes the total number of blocks in the Hamiltonians (corresponding to the number of d_j's). Dashed lines are included as guides for the eye. *Lower panels*: Decay of the ratios R_q^n for fixed system size $N = 12$, the largest size for which we computed the full spectrum. Solid lines are fits to the power-law function $f(n) = b/n^{a-1}$, with the extracted exponent satisfying $a \approx q$ up to small deviations. Panels on the left correspond to the Bethe Ansatz integrable case with $\alpha = 0$ and $\Delta = 0.1$, while panels on the right show the non-integrable case with $\alpha = 0.1$ and $\Delta = 0.1$.
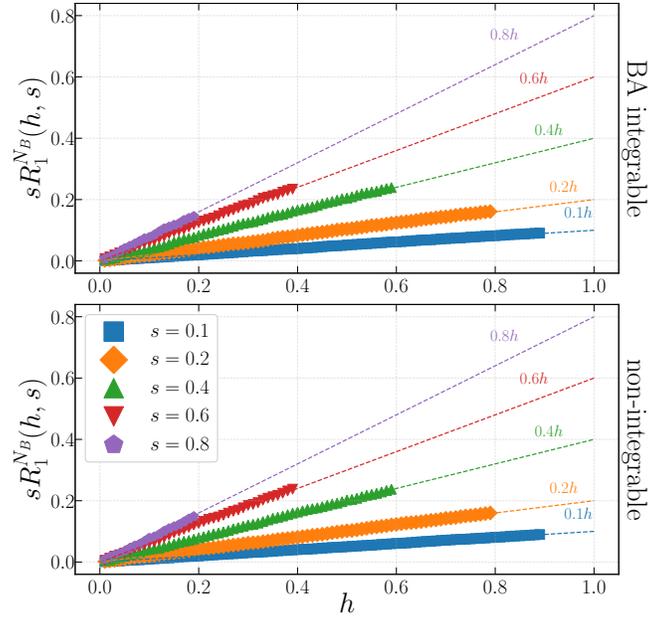
Figure 3. Numerical check of (12) for the paradigmatic example of a physical (local) Hamiltonian given by XXX+NNN chain in (21). We fix the system size $N = 12$, show the result of the quantity $sR_1^N(h, s)$ which is expected to be sh. *Upper panel*: Bethe Ansatz integrable case with $\alpha = 0$ and $\Delta = 0.1$. *Lower panel*: non-integrable case with parameters $\alpha = 0.1$ and $\Delta = 0.1$. Infinite temperature $T \to \infty$ regime.

2. Check of the Lyapunov condition in Eq. (12) at high temperature

We now turn to verifying condition (12) from the main text. By Theorem 3, this condition, together with the assumption of independence of the energy levels, guarantees that the associated random walk converges to a Wiener process in the thermodynamic limit. To recall, the condition requires that

$$\lim_{N \to \infty} R_1^N(h, s) = h \,, \tag{H3}$$

where we recall Eq. (C4):

$$R_q^N(h, s) := \frac{\sum_{k=\lfloor Ns \rfloor + 1}^{\lfloor N(s+h) \rfloor} d_k^{2q}}{\left(\sum_{k=1}^{N} d_k^2\right)^q} \,. \tag{H4}$$

In Fig. 3, we numerically plot $sR_1^N(h, s)$, which should asymptotically approach sh for large system sizes N, for various values of h and s. The results show excellent agreement with the theoretical prediction (dotted lines), confirming the expected behavior.

In summary, for the XXZ+NNN chain, we have verified that both Lyapunov-type conditions for the spectral weights—Eqns. (7) and (12)—are satisfied. These are necessary prerequisites for Theorems 2 and 3 to apply. What remains is the verification of linear independence of the energy spectrum over the rationals—a requirement that is, in practice, numerically intractable. Nevertheless, for non-integrable systems, spectral independence is generally expected. In contrast, the Bethe-Ansatz integrable case is more subtle: it may yield spectra that are either rationally independent or contain many rational relations.

3. Violation of the Lyapunov condition Eq. (7) at low temperature

In Fig. 4, we demonstrate the breakdown of the Lyapunov condition Eq. (7) at low temperature, thus signaling the inapplicability theorems 2 and 3. In particular, with the decrease of the temperature parameter T, we observe (from the top to bottom panels) that the ratio $R_q^{N_B}$ changes its exponential decay with the system size and flattens off as the zero temperature limit is approached.

4. Probability distribution of the spectral form factor $|\chi(t)|^2$

In Fig. 5, we show the full probability distribution of the normalized SFF, $|\chi(t)|^2/\overline{|\chi(t)|^2}$ both in the non-integrable and Bethe-Ansatz integrable phases of the XXZ+NNN chain (right panels). It is apparent that in both the Bethe-Ansatz and in the non-inegrable phases, the behavior of the SFF is the one predicted by Theorem 2: $|\chi(t)|^2/\overline{|\chi(t)|^2} \to \mathsf{Exp}(1)$ for increasing system size. It is interesting to notice, as shown in Table I, that the BA integrable regime cannot be differentiated from fully non-integrable theories by the long-time behavior of the SFF.

In Fig. 6 we demonstrate that quasi-free theories instead, exhibit a behavior of the SFF predicted by Theorem 5, i.e. the SFF is lognormal and its properly normalized logarithm becomes Gaussian in the thermodynamic limit. More precisely, using the notation of Theorem 5,

$$\frac{\log\left(|\chi(t)|^2\right)}{\sqrt{\sum_{j=1}^{L_B} g_j^2}} \to \mathsf{N}\left(0, \frac{\pi^2}{3}\right). \tag{H5}$$

To check Eq. (H5) we perform numerics on the XY model given by the following Hamiltonian

$$H_{XY} = -\sum_{i=1}^{L} \left[\left(\frac{1+\gamma}{2}\right) \sigma_i^x \sigma_{i+1}^x + \left(\frac{1-\gamma}{2}\right) \sigma_i^y \sigma_{i+1}^y + h\sigma_i^z\right]. \tag{H6}$$

We use periodic boundary conditions on the fermions (see e.g. [47] for a discussion). Standard diagonalization brings the model to

$$H_{XY} = \sum_{k \in BZ} \Lambda_k \left(\eta_k^\dagger \eta_k - \frac{1}{2}\right), \tag{H7}$$
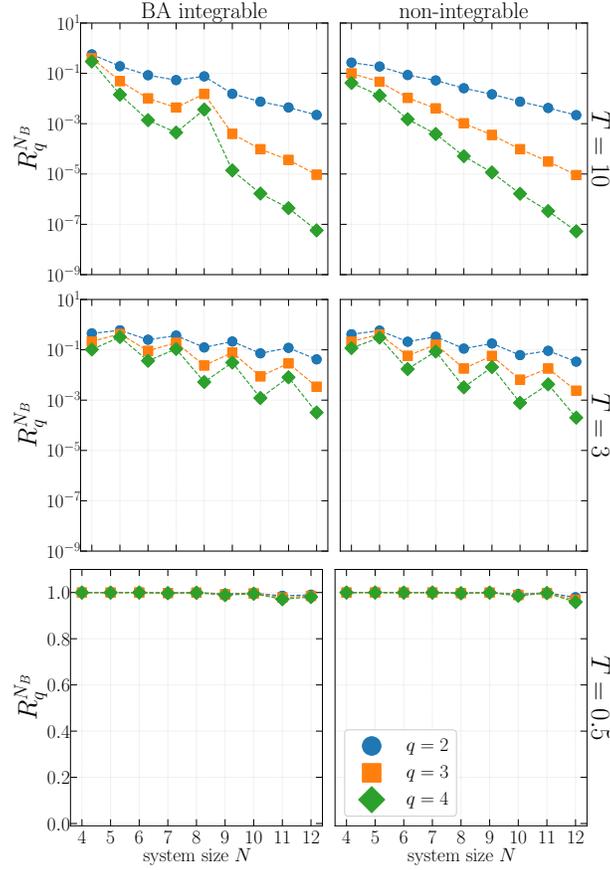
Figure 4. Numerical check of (7) for the paradigmatic example of a physical (local) Hamiltonian given by XXX+NNN chain in (21) at low and different temperatures T and breakdown of the Lyapunov conditions. Decay of the ratios $R_q^{N_B}$ for various system sizes N, where N_B denotes the total number of blocks in the Hamiltonians (corresponding to the number of d_j's). Dashed lines are included as guides for the eye. Significant deviation from an exponential decay of the ratios signals the breakdown of the generic condition. Decrease of the temperature from the top to the bottom panel shows how exactly the condition is not longer satisfied in the low temperature limit.

where the Brillouin zone is $BZ = \{k | k = 2\pi n/L,\, n = 0, 1, \ldots, L-1\}$ and the single particle dispersion reads

$$\Lambda_k = 2\sqrt{\gamma^2 + h^2 + (1 - \gamma^2)\cos(k)^2 + 2h\cos(k)}, \tag{H8}$$

so that the SFF reads (see the proof of Theorem 5)

$$|\chi(t)|^2 = \prod_{k=1}^{L} \left| 1 + e^{-it\Lambda_k} \right|^2 \tag{H9}$$

$$= \prod_{j=1}^{L_B} \left(2\cos(t\epsilon_j/2) \right)^{2g_j}.$$

For general values of h, γ, the one particle spectrum Λ_k is doubly degenerate so that $g_j = 2, \forall j$, and $L_B = L/2$. At the point $h = \gamma = 0$ the spectrum becomes $\Lambda_k = 2|\cos(k)|$. In this case, one can prove that ϵ_k is independent over the rationals for L a prime number, while it is expected not to be independent when L is not prime [48]. For other values of h, γ we observe the behavior expected from Theorem 5, irrespective if L is prime or not, indicating that the one particle spectrum is likely independent, see Fig. 6 upper panels. For $h = \gamma = 0$ the largest discrepancy from Eq. (H5) is expected when L is highly composite. So in the lower panels of Fig. 6 we show results for $L = 128 = 2^7$ which shows a large discrepancy (left) with those of $L = 127$ which is prime (right). See also [49] for analogous discussions on free fermionic spectra. Note that, for free theories the large parameter in the CLT is $L = \log_2(D)$, and the errors from applying the CLT at finite size are of the order of $O(L^{-1/2})$ as opposed to $O(D^{-1/2})$ for the non-integrable case. As a consequence, to check Theorem 2 for free models, we need to go to considerably larger sizes, while to check Theorem 5 in non-integrable models sizes of order of $L = 8$ suffice.
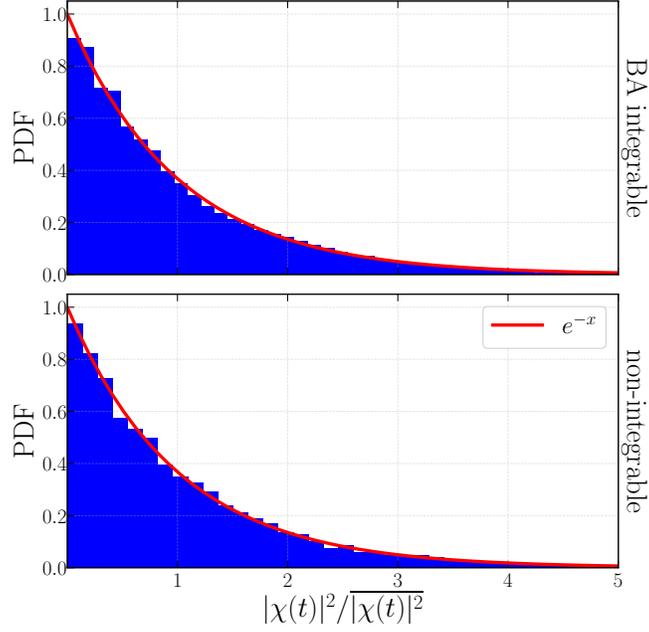
Figure 5. Probability distribution of the normalized Spectral Form Factor (SFF) for the XXZ + NNN chain spectrum at infinite temperature ($\rho = \mathbb{1}$) for system size $N = 8$. The distribution is obtained sampling in the time domain $[10^5, 2 \cdot 10^5]$. The prediction of Theorem 2, e^{-x}, is shown in red. *Upper panel*: non-integrable spectrum with $\Delta = 0.1$ and $\alpha = 0.1$. *Lower panel*: Bethe Ansatz integrable spectrum with $\Delta = 0.1$ and $\alpha = 0.0$. Notice the small system sizes used to perform the checks, and how well the exponential function captures the behavior.
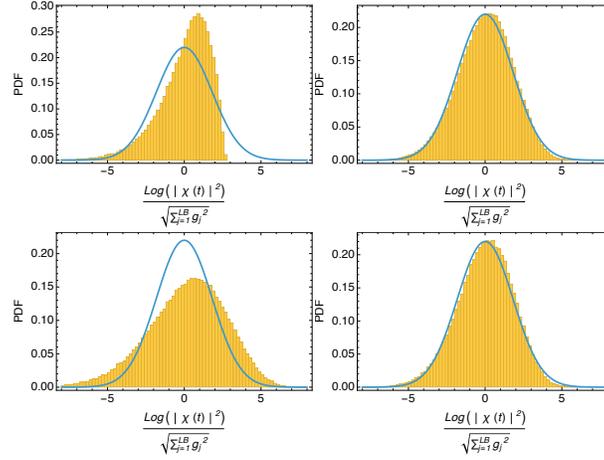
Figure 6. Check of Eq. (H5) for the free XY model. Upper panels: $(h, \gamma) = (0.2, 0.3)$ $L = 8$ (left panel) and $L = 170$ (right panel). Lower panels $(h, \gamma) = (0, 0)$ $L = 128$ (left panel) and $L = 127$, prime (right panel). The histograms are obtained sampling 2×10^5 time points uniformly in $[10^3, 2 \times 10^5]$.

5. SFF distribution and moments in the SYK model

We now turn to a random (disordered) model and, in particular, we consider the generalized Sachdev-Ye-Kitaev (SYK-k) model [50–52]. The SYK-k model describes a k-body all-to-all interaction between N Majorana fermionic modes. The Hamiltonian reads

$$H^{\text{SYK}-k} = (i)^{k/2} \sum_{1 \leq i_1 < \ldots < i_k \leq N} J_{i_1 i_2 \ldots i_k} \chi_{i_1} \chi_{i_2} \cdots \chi_{i_k} \tag{H10}$$
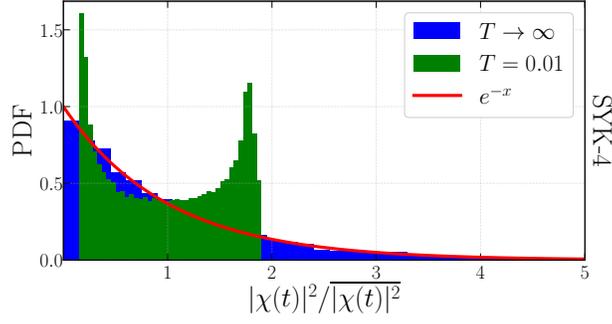
Figure 7. Probability density function (PDF) of the SFF at different temperatures for the SYK-4 model spectrum with $J = 1$ and $N = 18$ Majorana modes. Histograms of the SFF are obtained sampling 10^5 time points uniformly distributed in $[10^5, 2 \times 10^5]$ and and for a single realization of the disorder couplings.

	High Temperature $T = \infty$		Low Temperature $T = 0.01$	
	Gaussian (%)	Exact (%)	Gaussian (%)	Exact (%)
K_2	0.229	0.033	46.452	0.011
K_3	1.018	0.434	79.754	0.007
K_4	1.484	0.316	93.936	0.025

Table II. Relative errors (in percentages) of the moments of the SFF of the SYK-4 model between the exact formulae (average of) Eqns. (15) and the Gaussian approximation $K_m \simeq m!$. The numerical data are obtained by sampling t uniformly in $[10^5, 2 \times 10^5]$, 10^4 times and performing an additional ensemble average over 100 realizations for the SYK-4 model with $N = 18$ Majorana fermions. Increasing the number of realizations and time domain sampling leads to better agreement. The superior agreement of the exact expression is most evident for low temperatures.

with k being an even and positive integer number and χ_i Majorana operators. The couplings $J_{i_1,i_2,\ldots,i_k}$ are identical, independent distributed (i.i.d.) gaussian variables with mean and variance given by

$$\mathsf{E}[J_{i_1,i_2,\ldots,i_k}] = 0 \,, \quad \mathsf{E}[J^2_{i_1,i_2,\ldots,i_k}] = \frac{(k-1)!J}{N^{k-1}} \,. \tag{H11}$$

To perform exact diagonalization of the model and obtain its spectrum, we use the Jordan-Wigner transformation and map the Majorana operators into strings of Pauli operators [53, 54]. For $k = 2$, the model constitutes a random quadratic model that is not chaotic [55], while for $k \geq 4$, the model is considered strongly chaotic. The spectrum of SYK-4 is non-degenerate when $N \mod 8 = 0$ so that $d_j = 1 \; \forall j = 1, \ldots, D$, while it is entirely doubly degenerate, i.e. $d_j = 2, \; \forall j = 1, \ldots, N_B$ when $N \mod 8 \neq 0$ due to a particle-hole symmetry [17]. This implies that both Eqns. (7) and (12) are satisfied. The probability distribution of the eigenvalues is not known, but our numerical calculations and the computations in [33] suggest that it is absolutely continuous with respect to the Lebesgue measure. This would imply that, besides the known degeneracies for $N \mod 8 \neq 0$ that we mentioned, with probability one, the spectrum is independent. This implies that, at infinite temperature $\rho = \mathbb{I}$, all the Theorems 2, 3, and 4, apply to the SYK-4 model. At low enough temperature, the Lyapunov condition Eq. (7) is not satisfied. According to Theorem 2 the distribution of the random variable Y_n is no longer Gaussian in the thermodynamic limit, and, correspondingly, the distribution of $|\chi(t)|^2/\overline{|\chi(t)|^2}$ is no longer exponential.

In Fig. 7, we show the full probability distribution of the normalized SFF both at infinite temperature and at very low temperature. It is apparent that in the $T = \infty$ case the distribution is $\mathsf{Exp}(1)$ which follows from Theorem 2 while at $T = 0.01$ the distribution is double-peaked signaling a breakdown of the CLT.

In Table II we show analogous results for the normalized moments of the SFF, K_m, defined as

$$K_m = \frac{\mathsf{E}_x\left[\overline{|\chi(t)|^{2m}}\right]}{\left(\mathsf{E}_x\left[\overline{|\chi(t)|^2}\right]\right)^m} = \frac{\mathsf{E}_x\left[I_m\right]}{\left(\mathsf{E}_x[I_1]\right)^m} \,, \tag{H12}$$

where, to obtain better figures we also averaged over the random variables with E_x. The ensemble average of formulae Eqns. (16) and (17) give the correct moments while the Gaussian approximation $K_m \simeq m!$ fails at low temperature.

6. Evaluating the fractal dimension of the Brownian walker (or SFF) frontier

The fractal dimension is a quantitative measure that captures the complexity or "roughness" of a geometric object, especially those that exhibit self-similarity across scales. One widely used approach for estimating the fractal dimension is the *box-counting method*. This technique involves overlaying a grid of square boxes of side length ε over the domain containing the fractal and counting the number $N(\varepsilon)$ of boxes that intersect the fractal set. As $\varepsilon \to 0$, the fractal dimension d_F is estimated by analyzing the scaling behavior of $N(\varepsilon)$, typically through a log-log regression

$$d_F = \lim_{\varepsilon \to 0} \frac{\log N(\varepsilon)}{\log(1/\varepsilon)}. \tag{H13}$$

In practical implementations, this limit is approximated by evaluating $N(\varepsilon)$ at a range of decreasing box sizes and estimating the slope of the linear fit in a $\log$-$\log$ plot.

We verified that our implementation accurately reproduces a wide range of known fractal objects with exact dimensions in the range $0 < d_F < 2$. However, in realistic datasets that are not explicitly designed to exhibit fractal behavior (for example the Koch curve), there is some degree of arbitrariness in selecting the range of scales over which a clear power-law appears. Such is our case and the geometrical object that represent the fractal frontiers. To ensure statistical significance of our findings we preform the measurement of fractal dimension of the frontier on a ensemble of random walks (up to 20 different trajectories) for each of the considered regimes. Each member of the ensemble is generated by the same, exact, deterministic spectrum (in case of the disorder-free XXZ+NNN chain) but a different randomized value for the time parameter t sampled uniformly at random in $t \in [1, 2 \times 10^5]$.

Additionally, we note that isolating the fractal frontier in practice requires rasterizing numerical data into image format, a process that inherently reduces the precision of subsequent fractal dimension estimations. Extracting the frontier itself poses a significant technical challenge, as the random walker spans the continuous $\mathbb{R}^2$ plane. Standard convex hull algorithms, such as the gift wrapping algorithm [56], are not well-suited for capturing rugged, scale-invariant structures. If the walker were constrained on a lattice, we would see implementing such an algorithm worthwhile effort. In this work we employed a combination of approaches using open-source image editing tools such as GIMP [57], along with image processing functionalities of the routine ImageMeasurements provided by the ©Mathematica software.

In Fig. 8, we illustrate the box-counting method using a representative pair of random-walks: one from the non-integrable (chaotic) case, and the other from the integrable XY chain with parameters $(h, \gamma) = (0.2, 0.3)$. These examples serve to visually demonstrate the qualitative differences between the two regimes. To ensure the reliability of our findings, the main text reports results averaged over multiple random-walks.
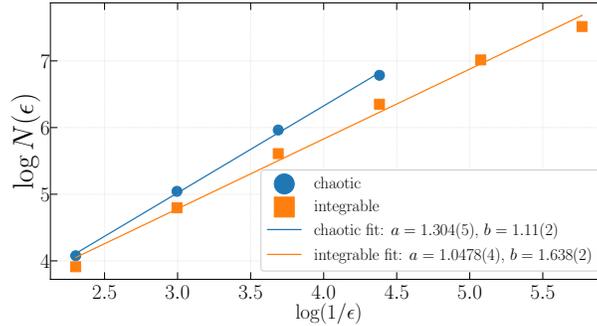
Figure 8. Box counting method and measurement of the fractal dimension for representative fractals. Straight lines are fits to the linear function $f(x) = ax + b$. The data reflects the frontier fractal dimension of the data presented in Fig. 1.

[1] J. L. Lagrange, Théorie des variations séculaires des éléments des planètes, Gauthier-Villars, Paris **V5**, 125 (1781), Œuvres, V5, Gauthier-Villars, Paris 1781, pp.125-207,.

[2] K. D. Schotte and U. Schotte, Tomonaga's Model and the Threshold Singularity of X-Ray Spectra of Metals, Phys. Rev. **182**, 479 (1969).

[3] A. Silva, Statistics of the Work Done on a Quantum Critical System by Quenching a Control Parameter, Phys. Rev. Lett. **101**, 120603 (2008).

[4] L. Campos Venuti and P. Zanardi, Unitary equilibrations: Probability distribution of the Loschmidt echo, Phys. Rev. A **81**, 022113 (2010).

[5] L. Campos Venuti, S. Yeshwanth, and S. Haas, Equilibration times in clean and noisy systems, Phys. Rev. A **87**, 032108 (2013).

[6] L. Campos Venuti and P. Zanardi, Universal time fluctuations in near-critical out-of-equilibrium quantum dynamics, Phys. Rev. E **89**, 022101 (2014).

[7] M. V. Berry, Semiclassical theory of spectral rigidity, Proceedings of the Royal Society of London. A. Mathematical and Physical Sciences **400**, 229 (1985), publisher: Royal Society.

[8] E. Brézin and S. Hikami, Spectral form factor in a random matrix theory, Phys. Rev. E **55**, 4067 (1997), publisher: American Physical Society.

[9] T. Prosen, Time Evolution of a Quantum Many-Body System: Transition from Integrability to Ergodicity in the Thermodynamic Limit, Phys. Rev. Lett. **80**, 1808 (1998), publisher: American Physical Society.

[10] T. Prosen, Ergodic properties of a generic nonintegrable quantum many-body system in the thermodynamic limit, Phys. Rev. E **60**, 3949 (1999), publisher: American Physical Society.

[11] H. Kunz, The probability distribution of the spectral form factor in random matrix theory, J. Phys. A: Math. Gen. **32**, 2171 (1999).

[12] J. Cotler, N. Hunter-Jones, J. Liu, and B. Yoshida, Chaos, complexity, and random matrices, J. High Energ. Phys. **2017** (11), 48.

[13] D. Roy and T. Prosen, Random matrix spectral form factor in kicked interacting fermionic chains, Phys. Rev. E **102**, 060202 (2020), publisher: American Physical Society.

[14] J. Šuntajs, T. Prosen, and L. Vidmar, Spectral properties of three-dimensional Anderson model, Annals of Physics Special issue on Philip W. Anderson, **435**, 168469 (2021).

[15] D. Roy, D. Mishra, and T. Prosen, Spectral form factor in a minimal bosonic model of many-body quantum chaos, Phys. Rev. E **106**, 024208 (2022), publisher: American Physical Society.

[16] A. Altland, F. Divi, T. Micklitz, S. Pappalardi, and M. Rezaei, Statistics of the Random Matrix Spectral Form Factor (2025), arXiv:2503.21386 [quant-ph].

[17] J. S. Cotler, G. Gur-Ari, M. Hanada, J. Polchinski, P. Saad, S. H. Shenker, D. Stanford, A. Streicher, and M. Tezuka, Black holes and random matrices, J. High Energ. Phys. **2017** (5), 118.

[18] E. Cáceres, A. Misobuchi, and A. Raz, Spectral form factor in sparse SYK models, J. High Energ. Phys. **2022** (8), 236.

[19] S. Choi, S. Kim, and J. Song, Supersymmetric Spectral Form Factor and Euclidean Black Holes, Phys. Rev. Lett. **131**, 151602 (2023), publisher: American Physical Society.

[20] J. Liu, Spectral form factors and late time quantum chaos, Phys. Rev. D **98**, 086026 (2018), publisher: American Physical Society.

[21] R. E. Prange, The Spectral Form Factor Is Not Self-Averaging, Phys. Rev. Lett. **78**, 2280 (1997), publisher: American Physical Society.

[22] Rayleigh, The problem of the random walk, Nature **72**, 318 (1905), publisher: Nature Publishing Group.

[23] K. Pearson, The problem of the random walk, Nature **72**, 342 (1905), publisher: Nature Publishing Group.

[24] F. Haake, *Quantum Signatures of Chaos* (Springer Science and Business Media, 2001).

[25] A. Flack, B. Bertini, and T. Prosen, Statistics of the spectral form factor in the self-dual kicked Ising model, Phys. Rev. Res. **2**, 043403 (2020), publisher: American Physical Society.

[26] J. Šuntajs, J. Bonča, T. Prosen, and L. Vidmar, Quantum chaos challenges many-body localization, Phys. Rev. E **102**, 062144 (2020), publisher: American Physical Society.

[27] A. Chan, A. De Luca, and J. T. Chalker, Spectral Lyapunov exponents in chaotic and localized many-body quantum systems, Phys. Rev. Res. **3**, 023118 (2021), publisher: American Physical Society.

[28] M. Winer and B. Swingle, Hydrodynamic Theory of the Connected Spectral form Factor, Phys. Rev. X **12**, 021009 (2022), publisher: American Physical Society.

[29] A. Legramandi and N. Talwar, The moments of the spectral form factor in SYK (2024), arXiv:2412.18737 [hep-th].

[30] V. Kumar, T. Prosen, and D. Roy, Leading and beyond leading-order spectral form factor in chaotic quantum many-body systems across all Dyson symmetry classes (2025), arXiv:2502.04152 [cond-mat].

[31] J. M. Borwein, D. Nuyens, A. Straub, and J. Wan, Some arithmetic properties of short random walk integrals, Ramanujan J **26**, 109 (2011).

[32] J. M. Borwein, A. Straub, J. Wan, W. Zudilin, and D. Zagier, Densities of short uniform random walks, Canadian Journal of Mathematics **64**, 961–990 (2012).

[33] A. M. García-García, Y. Jia, and J. J. M. Verbaarschot, Exact moments of the Sachdev-Ye-Kitaev model up to order $1/N^2$, J. High Energ. Phys. **2018** (4), 146.

[34] S. F. E. Oliviero, L. Leone, F. Caravelli, and A. Hamma, Random matrix theory of the isospectral twirling, SciPost Physics **10**, 076 (2021).

[35] K. J. Falconer, *The Geometry of Fractal Sets*, Cambridge Tracts in Mathematics (Cambridge University Press, Cambridge, 1985).

[36] B. B. Mandelbrot, *The Fractal Geometry of Nature*, 2nd ed. (Times Books, San Francisco, 1982).

[37] G. F. Lawler, O. Schramm, and W. Werner, The Dimension of the Planar Brownian Frontier is 4/3, Math. Res. Lett. **8**, 401 (2001), publisher: International Press of Boston.

[38] J. M. Deutsch, Quantum statistical mechanics in a closed system, Phys. Rev. A **43**, 2046 (1991).

[39] L. Campos Venuti and P. Zanardi, Theory of temporal fluctuations in isolated quantum systems, Int. J. Mod. Phys. B **29**, 1530008 (2015).

[40] L. Campos Venuti, Theory of Temporal Fluctuations in Isolated Quantum Systems, in *Quantum Criticality in Condensed Matter*, 50th Karpacz Winter School of Theoretical Physics, Karpacz, Poland, 2 – 9 March 2014 (World Scientific Publishing Company, 2015).

[41] H. A. Verrill, Sums of squares of binomial coefficients, with applications to Picard-Fuchs equations (2004), arXiv:math/0407327.

[42] H. A. Verrill, Root lattices and pencils of varieties, Journal of Mathematics of Kyoto University **36**, 423 (1996), publisher: Duke University Press.

[43] D. Szász-Schagrin, B. Pozsgay, and G. Takács, Weak integrability breaking and level spacing distribution, SciPost Physics **11**, 037 (2021).

[44] B. T. McDonough, C. Chamon, J. H. Wilson, and T. Iadecola, Bridging classical and quantum information scrambling with the operator entanglement spectrum (2025), arXiv:2505.05575 [quant-ph].

[45] A. Gu, S. F. E. Oliviero, and L. Leone, Doped stabilizer states in many-body physics and where to find them, Phys. Rev. A **110**, 062427 (2024).

[46] L. Leone, S. F. E. Oliviero, and A. Hamma, Isospectral twirling and quantum chaos, Entropy **23**, 10.3390/e23081073 (2021).

[47] L. Campos Venuti and M. Roncaglia, Equivalence between XY and dimerized models, Phys. Rev. A **81**, 060101 (2010).

[48] L. Campos Venuti, N. T. Jacobson, S. Santra, and P. Zanardi, Exact Infinite-Time Statistics of the Loschmidt Echo for a Quantum Quench, Phys. Rev. Lett. **107**, 010403 (2011).

[49] J. Riddell and B. Bertini, Rationally independent free fermions with local hopping, Physical Review E **110**, 064101 (2024), arXiv:2404.12100 [quant-ph].

[50] S. Sachdev and J. Ye, Gapless spin-fluid ground state in a random quantum Heisenberg magnet, Physical Review Letters **70**, 3339 (1993).

[51] A. Kitaev, Proceedings of the Kavli Institute for Theoretical Physics - KITP (2015), `http://online.kitp.ucsb.edu/online/entangled15/kitaev/`, `http://online.kitp.ucsb.edu/online/entangled15/kitaev2/`.

[52] B. Jasser, J. Odavić, and A. Hamma, Stabilizer entropy and entanglement complexity in the Sachdev-Ye-Kitaev model (2025), arXiv:2502.03093 [quant-ph].

[53] S. B. Bravyi and A. Kitaev, Fermionic quantum computation, Annals of Physics **298**, 210 (2002).

[54] G. Sarosi, AdS$_2$ holography and the SYK model, in *Proceedings of XIII Modave Summer School in Mathematical Physics - PoS (Modave2017)*, Vol. 323 (2018) p. 001.

[55] C. Liu, X. Chen, and L. Balents, Quantum entanglement of the Sachdev-Ye-Kitaev models, Physical Review B **97**, 245126 (2018).

[56] C. E. Leiserson, R. L. Rivest, and C. Stein, *Introduction to Algorithms, Second Edition*, 2nd ed., edited by T. H. Cormen (Mit Pr, Cambridge, Mass., 2001).

[57] The GIMP Development Team, Gnu image manipulation program (gimp), version 3.0.2. community, free software (license gplv3) (2025), version 3.0.2, Free Software.